Robotica (2003) volume 21, pp. 117–135. © 2003 Cambridge University Press
DOI: 10.1017/S0263574702004538 Printed in the United Kingdom

Noncollocated passivity-based PD control of a single-link flexible manipulator

Liang-Yih Liu and King Yuan*

Department of Mechanical Engineering, National Taiwan University, Taipei, Taiwan (R.O.C.)

(Received in Final Form: August 30, 2002)

SUMMARY

The passivity property of a noncollocated single-link flexible manipulator with a parameterized output is studied. The system can be characterized by either the irrational transfer function of an infinite-dimensional model or its truncated rational transfer functions. Necessary and sufficient conditions for these transfer functions to be passive are found. It is also shown that a non-passive, marginal minimum-phase, truncated transfer function can be rendered passive by using either the root strain feedback or the joint angular acceleration feedback. For the noncollocated truncated passive transfer function, a PD controller suffices to stabilize the overall system. Numerical results are given to show the efficacy of the proposed approaches.

KEYWORDS: Flexible manipulator; Noncollocated system; Feedback passivation; PD control.

1. INTRODUCTION

Flexible manipulators are inherently infinite-dimensional systems. In noncollocated control of a single-link flexible manipulator, the presence of an infinite number of right half-plane zeros in the transfer function from the joint torque to the tip position has long been recognized as the source of performance limitation due to the non-minimum phase nature of the open-loop system.[1,2] To cope with this difficulty, two approaches have been proposed in the literature. The first approach investigated by Park and Asada[3] involves the relocation of torque actuation by a torque transmission. Despite their complicated mechanical structure of the flexible arm, a minimum phase system can be attained only when the actuator and sensor are completely collocated at the tip point of the flexible link. Moreover, the conclusion was reached based on a finite dimensional model. A similar approach which considers the relocations of both the torque actuation point and the output measurement point along the link was studied by De Luca and Lanari[4] using a finite-dimensional model. Unfortunately, as the number of modes in the dynamic model increases, a minimum phase system is achieved still with the collocated situations.

The second approach is to use an output other than the actual tip position of the flexible link. These include the angular position of a point located on the link,[5] the joint angle plus a weighted value of tip deflection,[6,7] the reflected tip position,[8] the projection of the tip point on a rotating rigid axis[9] and the joint angle augmented with a weighted value of the slope of the link at its tip.[10] In most of these works,[5–8] however, the zeros were studied using finite-dimensional models. An important drawback of this finite-dimensional approach is that the minimum phase condition thus obtained is not always reliable. For example, the analysis performed by Spector and Flasher[2] using an infinite-dimensional model clearly rejects the validity of the results obtained in De Luca et al.[5] based on an approximate finite-dimensional model. Therefore, in order to establish the necessary and sufficient condition for a noncollocated single-link flexible manipulator to be minimum phase, there is no alternative but to resort to an accurate infinite-dimensional model of the flexible link. Several attempts[9,10] were made to find the minimum phase condition for some specific outputs using infinite-dimensional models. However, since the method used in these works[9,10] characterizes only the real positive zeros (leaving the unstable complex zeros completely ignored), the minimum phase condition thus obtained is only a necessary (but not sufficient) one.

In a recent work,[11] a linear infinite-dimensional model of the single-link flexible manipulator taking full account of the mass properties of the hub and tip payload was considered. With the joint torque as the input and the joint angle plus a weighted value of tip deflection as the measured output, an exact transfer function involving transcendental functions was derived. A necessary and sufficient condition in terms of the weighting factor k of tip deflection has been obtained such that the transfer function does not have any open right half-plane zeros. To be specific, the noncollocated single-link flexible system is at a margina1 minimum phase if and only if $-\infty<k<0.742$, where $k=1$ corresponds to the actual tip point of the link. However, a passivity analysis was not considered therein.

On the other hand, it was first demonstrated by Wang and Vidyasagar[12] that for a link with sufficiently small hub inertia (relative to the beam inertia), the transfer function from the joint torque to the reflected tip velocity based on a finite-dimensional model is passive. Based on the passivity theorem,[13] a strictly passive output feedback controller with finite gain stabilizes any passive system in an L_2 sense. This implies that very simple controllers can be designed for the passive system. Note that the transfer function considered by Wang and Vidyasagar[12] is only a truncated approximation of the aforementioned linear infinite-dimensional model[11] with an additional constraint $k=-1$.

Motivated by the desirability of passivity property of a transfer function, several questions naturally arise as follows. First, what is the necessary and sufficient condition

https://doi.org/10.1017/S0263574702004538 Published online by Cambridge University Press

for the general linear infinite dimensional model[11] to be passive? Second, if a finite-dimensional truncated model is useful for practical applications, can the passivity property be achieved through the adjustment of system parameters? Third, for a nonpassive truncated transfer function, can it be rendered passive by using an output feedback? The goal of this paper is intended to answer these questions. A linear infinite dimensional model of the single-link flexible manipulator studied by Yuan and Liu[11] with a parameterized output will be used as a starting point. For simplicity, the tip payload is neglected. Since the minimum phase property is a necessary condition for a transfer function to be passive, a small relevant part of the minimum phase analysis performed in Yuan and Liu[11] is reproduced here for the sake of completeness. The interlacing property[14] of the poles and zeros on the imaginary axis is used to establish the necessary and sufficient condition for a transfer function to be passive. If a minimum phase truncated transfer function is not passive, it will be shown that either the root strain feedback or the joint angular acceleration feedback can render the closed-loop transfer function passive. Thus, the remaining problem is to design an additional controller for the noncollocated truncated passive system. The PD controller which was originally established by Gevarter[15] for the stabilization of collocated truncated transfer functions will be proved to be readily applicable for the noncollocated truncated passive transfer functions. Numerical results are given to show the efficacy of the above proposed approaches.

2. DYNAMIC MODEL

Consider the horizontal motion of a single-link flexible manipulator with a free tip end as shown in Figure 1. The link is assumed to be a uniform, homogeneous, Euler-Bernoulli beam of length ℓ, mass per unit length ρ, and flexural rigidity EI. The hub is modelled by a single-mass moment of inertia I_h, where the driving torque $\tau(t)$ is applied. Also shown in Figure 1, $\theta(t)$ designates the hub rotation angle, and $v(x, t)$ denotes the small elastic deflection of the link. Introducing the new variable $w(x, t)$ such that[1]

$$w(x, t)=x\theta(t)+v(x, t), \tag{1}$$

then the equations of motion and its corresponding boundary conditions can be written as[1,16]

$$\rho\ddot{w}(x, t)+EIW_{xxxx}(x, t)=0, \tag{2}$$

$$w(0, t)=0, \qquad w_x(0, t)=\theta(t), \tag{3}$$

$$\mathrm{w}_{xx}(\ell, t)=0, \qquad w_{xxx}(\ell, t)=0, \tag{4}$$

$$I_h\ddot{\theta}(t)=\tau(t)+EIw_{xx}(0, t), \tag{5}$$

where $\dot{(\ )}$ and $(\ )_x$ denote $\frac{\partial}{\partial t}$ and $\frac{\partial}{\partial x}$, respectively.

2.1. Noncollocated minimum phase open-loop transfer function

It is known[1] that the transfer function from the input torque $\tau(t)$ to the actual tip position $w(\ell, t)=\ell\theta(t)+v(\ell, t)$ is a nonminimum phase. To remedy this difficulty, let the output be chosen as $y(t)=w(\ell, t)+(k-1)v(\ell, t)$, that is

$$y(t)=\ell\theta(t)+kv(\ell, t), \tag{6}$$

where k is a real parameter whose permissible values will be determined to satisfy the minimum phase condition. This, in a control context, is to change the zeros of $w(\ell, s)/\tau(s)$ to the zeros of $y(s)/\tau(s)$ by a parallel compensator $(k-1)v(\ell, s)/\tau(s)$, where s is the Laplace transform variable. Note that equation (6) includes the joint angle output ($k=0$), the tip position output ($k=1$), and the reflected tip position output[8] ($k=-1$) as special cases. Using equation (1), $y(t)$ can also be expressed in terms of $w(\ell, t)$ and $\theta(t)$ as

$$y(t)=(1-k)\ell\theta(t)+kw(\ell, t). \tag{7}$$

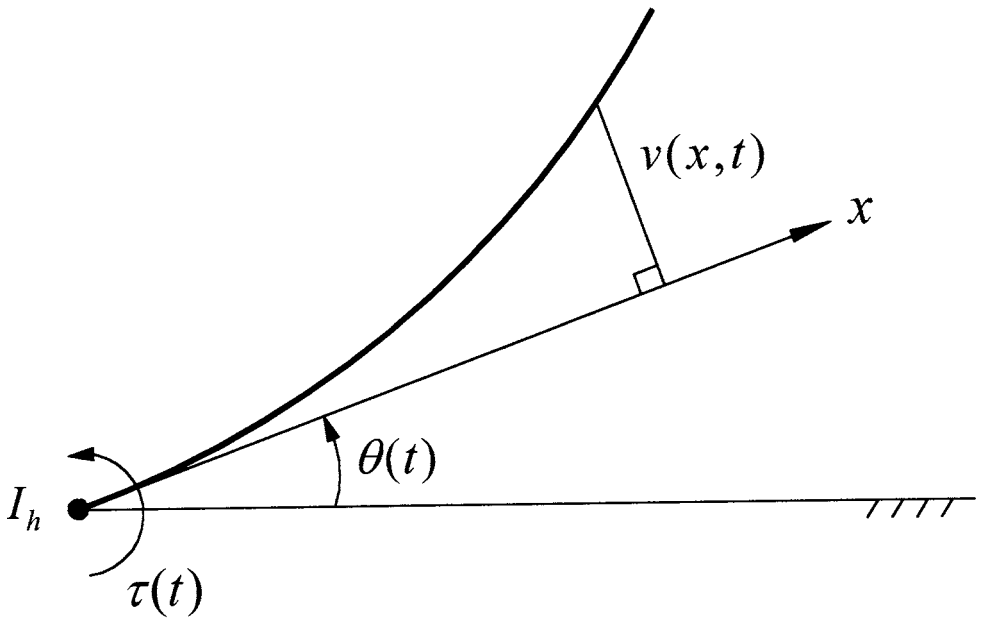


Fig. 1. Schematic of a single-link flexible manipulator.

https://doi.org/10.1017/S0263574702004538 Published online by Cambridge University Press

The transfer function between $\tau(t)$ and $y(t)$ can be derived by taking Laplace transform of equations (2)–(5) and (7) with zero initial conditions. Define the dimensionless parameters, β, ε and $\hat{s}$ as

$$\beta^4 = -\frac{\rho \ell^4}{EI} s^2 = -\hat{s}^2, \qquad \varepsilon = \frac{I_h}{\rho \ell^3}. \tag{8}$$

After tedious algebraic manipulations, the open-loop transfer function can be written as

$$G(\hat{s}, k, \varepsilon) := \frac{y(\hat{s})}{\tau(\hat{s})} = \frac{\ell^2}{EI} \cdot \frac{Z(\beta, k)}{P(\beta, \varepsilon)}, \tag{9}$$

where

$$Z(\beta, k) = (1-k)(1+\cosh\beta\cos\beta) + k\beta^{-1}(\sinh\beta + \sin\beta), \tag{10}$$

$$P(\beta, \varepsilon) = \beta(\sinh\beta\cos\beta - \cosh\beta\sin\beta) - \varepsilon\beta^4(1+\cosh\beta\cos\beta). \tag{11}$$

The detailed derivation of equation (9) and other transfer functions used in this work are outlined in Appendix A. Note that if $\beta = \sqrt{\omega}$ is a root of $P(\beta, \varepsilon) = 0$ (or $Z(\beta, k) = 0$), where ω is a real positive constant, then so are $-\sqrt{\omega}$ and $\pm j\sqrt{\omega}$. By using the equation $\beta^4 = -\hat{s}^2$, each of the four β roots maps into $\hat{s} = \pm j\omega$. Therefore, in order for $P(\beta, \varepsilon) = 0$ (or $Z(\beta, k) = 0$) to have roots on the imaginary $\hat{s}$-axis, it is sufficient to search for the real positive roots of $P(\beta, \varepsilon) = 0$ (or $Z(\beta, k) = 0$). To preserve the exact poles and zeros of $G(\hat{s}, k, \varepsilon)$, the product series expansions of $P(\beta, \varepsilon)$ and $Z(\beta, k)$ can be used. The infinite product expansions[2,17] of transcendental functions involved in equations (10)–(11) are particularly useful, and are summarized in Appendix B for reference. The convergence of such infinite product expansions is assured by the Mittag-Leffler theorem.[18]

It is known[19] that $G(\hat{s}, k, \varepsilon)$ has poles only on the imaginary $\hat{s}$-axis. For a given value of $\varepsilon \geq 0$, the equation $P(\beta, \varepsilon) = 0$ has four roots at $\beta = 0$ and a countable infinity of real positive roots $0 < \beta_1 < \beta_2 < \cdots \beta_n < \cdots (\lim_{n\to\infty} \beta_n \to \infty)$. Therefore, the poles of $G(\hat{s}, k, \varepsilon)$ are given by the rigid body modes at $\hat{s} = 0, 0$ and the flexible modes at $\hat{s} = \pm j\omega_{\theta n}(\varepsilon)$, where $\omega_{\theta n}(\varepsilon) = \beta_n^2(\varepsilon)$, $n = 1, 2\cdots$. Selected values of $\omega_{\theta n}$ thus computed numerically are shown in Table I. Using A2 and A3 from Appendix B, the poles of $G(\hat{s}, k, \varepsilon)$ can also be expressed as the roots of the following equation:

$$P(\hat{s}, \varepsilon) = \frac{2}{3}\hat{s}^2\left[\prod_{n=1}^{\infty}\left(1 + \frac{\hat{s}^2}{\omega_{\beta n}^2}\right) + 3\varepsilon\prod_{n=1}^{\infty}\left(1 + \frac{\hat{s}^2}{\omega_{pn}^2}\right)\right] = 0, \tag{12}$$

where $\omega_{\beta n}$ and ω_{pn} correspond to the well-known pinned-free and clamped-free bending vibration modes, respectively. Note from A2 and A3 of Appendix B that the interlacing property $\omega_{p,n+1} > \omega_{\beta n} > \omega_{pn} > 0$ holds for all $n \geq 1$ and that $\omega_{\beta n} \to \left(n + \frac{1}{4}\right)^2 \pi^2$ and $\omega_{pm} \to \left(n - \frac{1}{2}\right)^2 \pi^2$ as $n \to \infty$.

The poles $\hat{s} = \pm j\omega_{\theta n}$, $n = 1, 2\cdots$, moves along the imaginary $\hat{s}$-axis from $\pm j\omega_{\beta n}$ to $\pm j\omega_{pn}$ as ε increases from 0 to ∞ (see Table I and Figure 3). Using equation (12), $P(\hat{s}, \varepsilon)$ can be expressed as

$$P(\hat{s}, \varepsilon) = \frac{2}{3}(1+3\varepsilon)\hat{s}^2\prod_{n=1}^{\infty}\left(1 + \frac{\hat{s}^2}{\omega_{\theta n}^2}\right). \tag{13}$$

In what follows, the objective is to find the range of values of k such that $G(\hat{s}, k, \varepsilon)$ is minimum-phase. This is done by finding the zeros of equation (10). Using A1 and A2 from Appendix B, equation (10) can be expressed as

$$Z(\hat{s}, k) = 2\left[(1-k)\prod_{n=1}^{\infty}\left(1 + \frac{\hat{s}^2}{\omega_{pn}^2}\right) + k\prod_{n=1}^{\infty}\left(1 - \frac{\hat{s}^2}{\omega_{zn}^2}\right)\right] = 0. \tag{14}$$

The root locus of equation (14) is shown in Figure 2 based on a 6 pole-zero pair approximation. The approximate breakaway points on the imaginary $\hat{s}$-axis are $\pm 12.20j$, $\pm 92.10j$, $\pm 260.66j$ corresponding to $k = 0.759, 0.918, 0.984$, respectively. Note that the breakaway points on the imaginary $\hat{s}$-axis actually correspond to the real positive

Table I. Selected values of $\sqrt{\omega_{\theta n}(\varepsilon)}$.

Value of ε	Mode number n							
	1	2	3	4	5	6	7	8
0.0	3.927	7.069	10.210	13.352	16.493	19.635	22.777	25.918
0.01	3.641	5.616	8.084	11.075	14.174	17.298	20.432	23.570
0.05	2.968	4.897	7.897	11.011	14.144	17.283	20.423	23.563
0.1	2.639	4.794	7.876	11.003	14.141	17.281	20.422	23.563
1.0	2.010	4.704	7.857	10.996	14.138	17.279	20.420	23.562
10.0	1.890	4.695	7.855	10.996	14.137	17.279	20.420	23.562
100.0	1.877	4.694	7.855	10.996	14.137	17.279	20.420	23.562
∞	1.875	4.694	7.855	10.996	14.137	17.279	20.420	23.562

https://doi.org/10.1017/S0263574702004538 Published online by Cambridge University Press

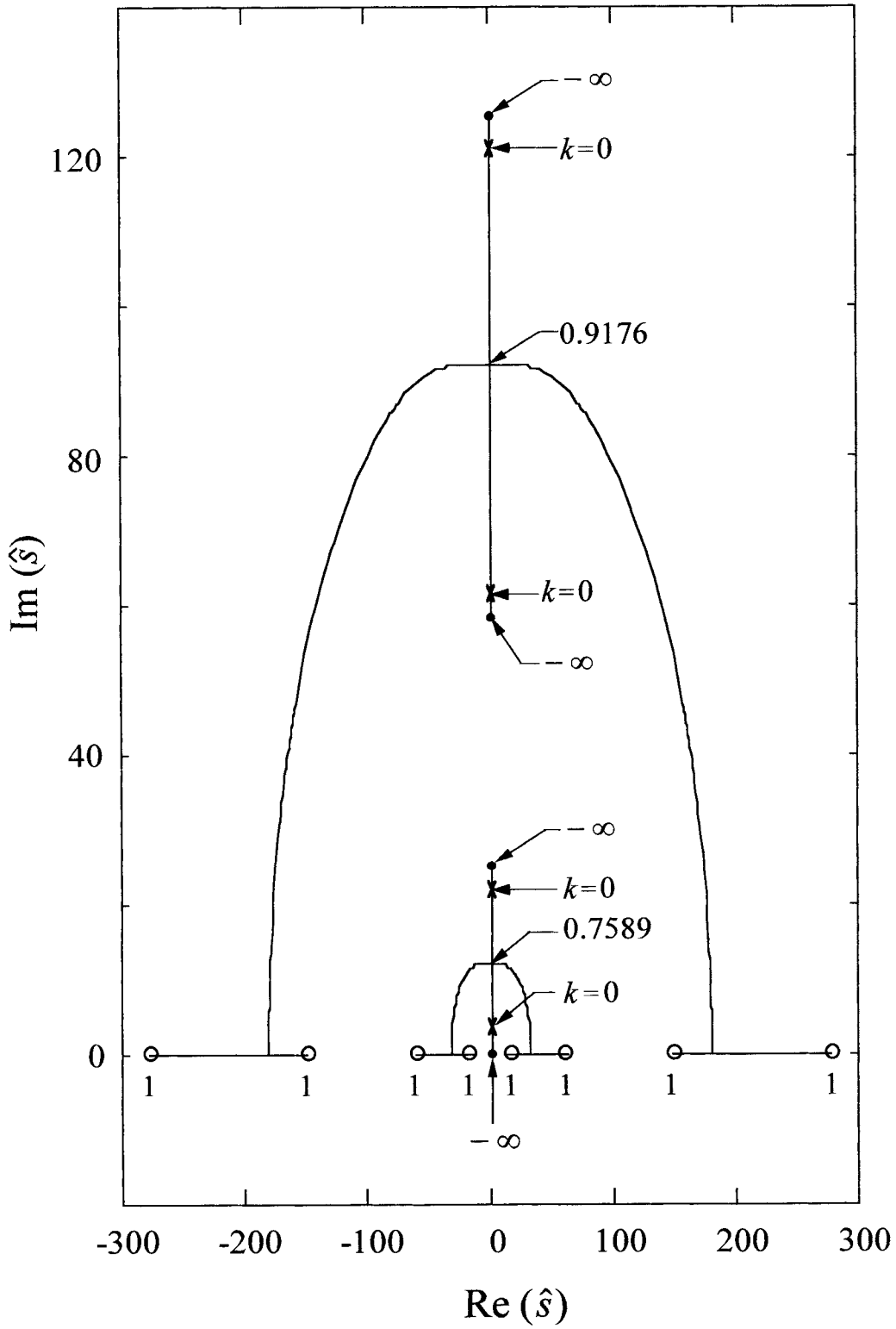


Fig. 2. Root locus of equation (14) for $-\infty<k<1$ using 6 pole-zero pairs approximation.

double zeros of equation (10). Numerical solutions[11] of $Z(\beta, k)=0$ reveal that there are no real positive double roots so long as $k<0.758$. Therefore, the infinite number of zeros of $G(\hat{s}, k, \varepsilon)$ will lie completely on the imaginary $\hat{s}$-axis if and only if $-\infty<k\leq 0.758$. Stated differently, the necessary and sufficient condition for $G(\hat{s}, k, \varepsilon)$ to be marginal minimum-phase is $-\infty<k\leq 0.758$. Previous studies,[6,7] on the minimum-phase condition which were obtained using approximate finite dimensional models yield different results depending on the number of modes included in the approximate modes. Let $\hat{s}=\pm j\omega_{\alpha n}(k)$ denote the imaginary roots of equation (14) for $k<0.758$. Then $Z(\hat{s}, k)$ can be recast as

$$Z(\hat{s}, k)=2\prod_{n=1}^{\infty}\left(1+\frac{\hat{s}^2}{\omega_{\alpha n}^2}\right). \tag{15}$$

https://doi.org/10.1017/S0263574702004538 Published online by Cambridge University Press

Table II. Selected values of $\sqrt{\omega_{\alpha n}(k)}$.

Value of k	Mode number n							
	1	2	3	4	5	6	7	8
$-\infty$	0.000	4.900	7.725	11.086	14.066	17.336	20.371	23.604
−100.0	0.573	4.900	7.726	11.085	14.067	17.336	20.372	23.604
−10.0	1.001	4.881	7.737	11.078	14.073	17.331	20.376	23.600
−1.0	1.551	4.798	7.791	11.041	14.102	17.308	20.396	23.583
−0.7	1.620	4.780	7.802	11.033	14.108	17.303	20.400	23.579
−0.5	1.676	4.764	7.812	11.026	14.114	17.298	20.404	23.576
−0.3	1.742	4.743	7.825	11.016	14.121	17.292	20.409	23.572
0.0	1.875	4.694	7.855	10.996	14.137	17.279	20.420	23.562
+0.3	2.082	4.601	7.909	10.956	14.167	17.254	20.441	23.544
+0.5	2.318	4.468	7.980	10.904	14.208	17.221	20.469	23.519
+0.7	2.847	4.082	8.145	10.777	14.301	17.142	20.534	23.462
+0.73	3.029	3.927	8.191	10.741	14.327	17.120	20.552	23.447
+0.742	3.142	3.825	8.213	10.724	14.339	17.110	20.561	23.439
+0.758	3.491	3.491	8.245	10.698	14.357	17.094	20.573	23.428

The numerical values of $\omega_{\alpha n}(k)$ can be computed using $\omega_{\alpha n}=\beta_n^2$ where $\beta_n(k)$ are the roots of $Z(\beta, k)=0$. Selected values of $\omega_{\alpha n}$ are shown in Table II. Since the asymptotic behavior of $Z(\beta, k)=0$, for $-\infty<k<0.758$ is governed[11] by $\cos\beta=0$, hence $\omega_{\alpha n}\rightarrow\left(n-\frac{1}{2}\right)^2\pi^2$ as $n\rightarrow\infty$. We emphasize here that the necessary and sufficient condition for $G(\hat{s}, k, \varepsilon)$ to be marginal minimum phase was obtained via the numerical solutions of the exact transcendental equation $Z(\beta, k)=0$, not by the finite-dimensional approximation of the root locus.

For the noncollocated marginal minimum phase transfer function $G(\hat{s}, k, \varepsilon)$, exact tracking of the output $y(t)$ with internal stability is achievable using the standard input-output inversion control techniques.[4,20] However, it would require full state observation of the distributed flexible variables which is not practically feasible. From the standpoint of cheap implementation, it will be interesting to discuss the possibility of using a PD controller to control the noncollocated marginal minimum phase transfer function. It has been shown[21] that if the noncollocated marginal minimum-phase *truncated* transfer function $\hat{s}G^*(\hat{s}, -1, \varepsilon)$ of a finite-dimensional model of the single-link flexible manipulator is passive for sufficiently small ε^*, then a PD-like controller asymptotically stabilizes $G^*(\hat{s}, -1, \varepsilon^*)$. A systematic generalization of the above work to the non-collocated marginal minimum-phase *irrational* transfer function $\hat{s}G(\hat{s}, k, \varepsilon)$ for $-\infty<k\leq 0.758$ and $\varepsilon\geq 0$ will be discussed in the sequel.

2.2. *Noncollocated passive open-loop transfer function*

Recall[14] that a rational transfer function $\hat{s}G^*(\hat{s})$ with a simple pole at the origin is passive if all its poles and zeros lie on the imaginary $\hat{s}$-axis and are distinct and alternate each other. This is the so-called interlacing property. In what follows, we generalize this property for an irrational marginal minimum phase transfer function $\hat{s}G(\hat{s})$. To this end, $\hat{s}G(\hat{s})$ can be expressed as

$$\hat{s}G(\hat{s})=\frac{K\prod_{n=1}^{N}\left(1+\frac{\hat{s}^2}{z_n^2}\right)}{\hat{s}\prod_{n=1}^{N}\left(1+\frac{\hat{s}^2}{p_n^2}\right)}=\frac{A_0}{\hat{s}}+\sum_{i=1}^{N}\frac{A_i\hat{s}}{\hat{s}^2+p_i^2}, \tag{16}$$

where by assumption $n\rightarrow\infty$, $K>0$, $0<z_1<z_2<\cdots<z_N<\cdots$, and $0<p_1<p_2<\cdots<p_N<\cdots$. It can be easily shown that

$$A_0=K>0, \tag{17}$$

$$A_i=-\frac{K}{p_i^2}\prod_{n=1}^{N}\left(\frac{p_n}{z_n}\right)^2\frac{\prod_{n=1}^{N}(z_n^2-p_i^2)}{\prod_{\substack{n=1\\n\neq i}}^{N}(p_n^2-p_i^2)}, \qquad i=1, 2, \cdots, N, \tag{18}$$

$$\mathrm{Re}[(\sigma\pm j\omega)G(\sigma\pm j\omega)]=\sigma\left\{\frac{A_0}{\sigma^2+\omega^2}+\sum_{n=1}^{\infty}\frac{A_i(\sigma^2+\omega^2+p_i^2)}{[\sigma^2+(\omega+p_i)^2][\sigma^2+(\omega-p_i)^2]}\right\}. \tag{19}$$

By definition, an irrational transfer function $H(s)$ is positive real[22] or passive if (i) $H(s)$ is analytic in $\mathrm{Re}(s)>0$, (ii) $H(s)$ is real for positive real s, and (iii) $\mathrm{Re}[H(\sigma\pm j\omega)]\geq 0$ for all $\sigma>0$. Therefore, $\hat{s}G(\hat{s})$ defined by equation (16) is passive for $N=1, 2, \cdots, \infty$ iff $A_0>0$ and $A_i>0$ for $i=1, 2, \cdots (\lim_{N\rightarrow\infty} A_N=0)$. We now proceed to prove the assertion by induction that if $A_i>0$, $i=1, 2, \cdots (\lim_{N\rightarrow\infty} A_N=0)$, then the interlacing property holds for $\hat{s}G(\hat{s})$. Referring to equation (16), it can be easily shown using equation (18) that (i) for $N=1$, $A_1>0$ implies $z_1<p_1$, and (ii) for $N=2$ and

https://doi.org/10.1017/S0263574702004538 Published online by Cambridge University Press

$z_1<p_1, A_1>0$ implies $p_1<z_2$ and $A_2>0$ implies $z_2<p_2$. Assume that for each positive integer N, $A_i>0$, $i=1, 2, \cdots, N$ imply $0<z_1<p_1<z_2<p_2<\cdots<z_N<p_N$. Then for the positive integer $N+1$, it can be shown using equation (18) that $A_i>0$, $i=1, 2, \cdots, N$ imply $p_N<z_{N+1}$ and $A_{N+1}>0$ implies $z_{N+1}<p_{N+1}$. This proves the above assertion for all $N=1, 2, \cdots, \infty$.

The interlacing property is now used to find the restrictions on k and ε such that the irrational marginal minimum phase transfer function $\hat{s}G(\hat{s}, k, \varepsilon)$ is passive. Figure 3 shows the distribution of poles $\pm j\omega_{\theta n}(\varepsilon)$ and zeros $\pm j\omega_{\alpha n}(k)$ of $G(\hat{s}, k, \varepsilon)$ on the imaginary $\hat{s}$-axis. For each value of $k<0.758$, there is one pole in each shaded strip (besides the double pole at $\hat{s}=0$), and one zero on each dashed line. To exclude $k=0.758$ is because the first zero $+j\omega_{\alpha 1}$ and the second zero $+j\omega_{\alpha 2}$ merge into one point there. As seen in Figure 3, to include the infinite number of flexible modes in $\hat{s}G(\hat{s}, k, \varepsilon)$, the interlacing property cannot

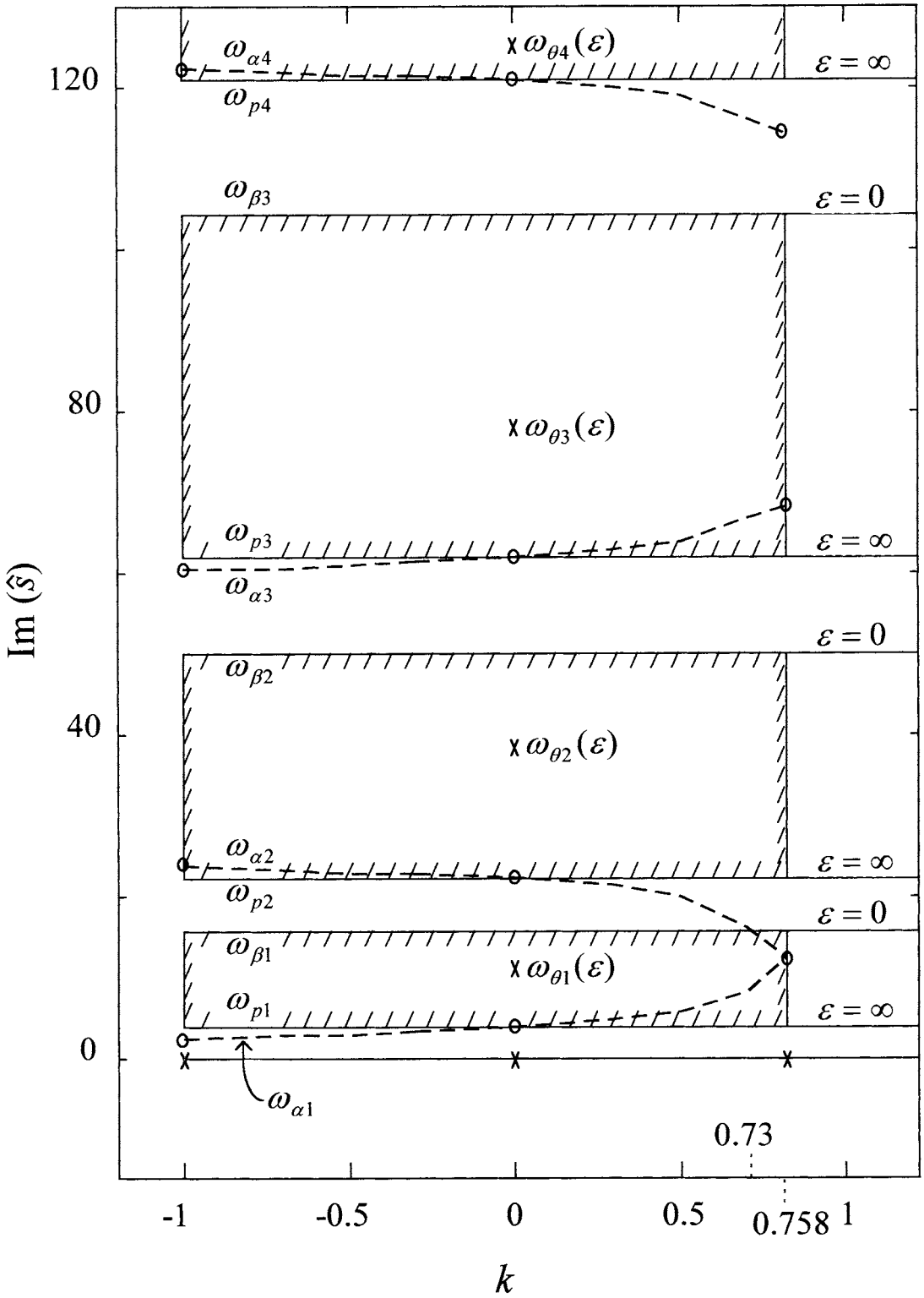


Fig. 3. Distribution of poles $\hat{s}=\pm j\omega_{\theta n}(\varepsilon)$ and zeros $\hat{s}=\pm j\omega_{\alpha n}(k)$ of $G(\hat{s}, k, \varepsilon)$ on the imaginary $\hat{s}$-axis.

https://doi.org/10.1017/S0263574702004538 Published online by Cambridge University Press

be achieved if neither (a) $k=0$, $0\le\varepsilon<\infty$, nor (b) $\varepsilon=0$, $-\infty<k<0.730$ is satisfied. For the case (a), we have from equation (14) that $\omega_{\alpha n}=\omega_{pn}$ because of $k=0$, and from equation (12) and Figure 3 that $\omega_{pn}<\omega_{\theta n}\le\omega_{\beta n}$. Recall also from Section 2.1 the asymptotic properties $\omega_{\beta n}=\left(n+\frac{1}{4}\right)^2\pi^2$ and $\omega_{p,n+1}=\left(n+\frac{1}{2}\right)^2\pi^2$ for $n\gg 1$, we conclude that the interlacing property $\omega_{\alpha n}<\omega_{\theta n}<\omega_{\alpha,n+1}<\omega_{\theta,n+1}$ for $n=1, 2\cdots$ is indeed true for the case (a). As for the case (b), we have from equation (12) that $\omega_{\theta n}=\omega_{\beta n}$ on account of $\varepsilon=0$, and from the numerical solutions of equation (14) and Figure 3 that $\omega_{\alpha n}<\omega_{\beta n}<\omega_{\alpha,n+1}$ for $n\le 8$. Recall also from Section 2.1 the asymptotic properties $\omega_{\alpha,n+1}=\left(n+\frac{1}{2}\right)^2\pi^2$ and $\omega_{\beta,n+1}=\left(n+\frac{5}{4}\right)^2\pi^2$ for $n\gg 1$, we conclude that the interlacing property also holds for the case (b). The restriction that $k\neq 0.730$ for the case $\varepsilon=0$ is due to the cancellation of first pole $\pm j\omega_{\beta 1}$ and the second zero $\pm j\omega_{\alpha 2}$ at $k=0.730$. In the general case, passivity can be achieved only for a truncated transfer function. However, the number of flexible modes N allowed for $\hat{s}G^*(\hat{s}, k, \varepsilon)$ to be passive depends on the values of k and ε. This is demonstrated in Table III. For $0.730<k<0.758$, passivity is still possible in a very narrow range of $0<\varepsilon_{\min}<\varepsilon<\varepsilon_{\max}<\infty$. It is not shown here due to its lack of practical significance. Note that the one flexible mode ($N=1$) truncated transfer function is always passive for a negative value of k. A passive truncated transfer function admitting higher order flexible modes usually restricts to sufficiently small value of ε for $k\neq 0$. From a control point of view, the higher order flexible modes are of limited significance because of their relatively large internal damping ratio, and also due to the finite bandwidth of the actuator. Thus, a passive truncated transfer function $\hat{s}G^*(\hat{s}, k, \varepsilon)$ still has great practical value since a flexible manipulator with a small but nonzero ε can always be constructed through mechanical design. Furthermore, a non-passive marginal minimum phase truncated transfer function may be rendered passive by using an appropriate output feedback. For notational simplicity, we use $\hat{s}G(\hat{s}, k, \varepsilon)$ to denote a marginal minimum phase *truncated* transfer function in the next section. For $k<0.730$, the substitution of equations (13) and (15) into (9) yields

$$\hat{s}G(\hat{s}, k, \varepsilon)=\frac{3\ell^2}{(1+3\varepsilon)EI}\cdot\frac{\prod_{n=1}^{N}\left(1+\frac{\hat{s}^2}{\omega_{\alpha n}^2}\right)}{\hat{s}\prod_{n=1}^{N}\left(1+\frac{\hat{s}^2}{\omega_{\theta n}^2}\right)}, \qquad (20)$$

where $0<\omega_{\alpha 1}<\omega_{\theta 1}<\cdots<\omega_{\alpha N}<\omega_{\theta N}$. Note that, owing to the infinite product representation of transfer function, the exact poles and zeros based on the original infinite dimensional model are preserved in all its truncated approximate models.

3. CONTROLLER DESIGN

As noted previously,[12] the passivity property of $\hat{s}G(\hat{s}, k, \varepsilon)$ permits the design of a large family of stabilizing controllers. In order to apply the passivity theorem, the plant must be chosen as $\hat{s}G(\hat{s}, k, \varepsilon)$ so that it has a relative degree one. Early attempts to design strictly passive controllers using the plant $\hat{s}G(\hat{s}, k, \varepsilon)$ included constant gain,[12] PI,[22] PD-like,[21] and lead compensator.[24] Note that the output of the plant $\hat{s}G(\hat{s}, k, \varepsilon)$ is $\dot{y}(t, k, \varepsilon)$. One cannot ensure that $y(t, k, \varepsilon)$ approaches a desired $y_d(t)$ without a steady-state error. To avoid the above difficulty, the control structure as shown in Figure 4 will be adopted in the subsequent discussion. Note that this control structure cannot be regarded as a PI controller for $\hat{s}G(s)$ because $y(t)$ then becomes unobservable from the output of $\hat{s}G(\hat{s})$. The major motivation of using this control structure is that it is straightforward to perform feedback passivation as well as the stability proof for a truncated passive system using a feedforward PD controller.

3.1. Stabilization of truncated passive $\hat{s}G(\hat{s}, k, \varepsilon)$ using PD controller

Consider the system shown in Figure 4, where K, z_n, p_n, k_p and k_d are positive constants. A theorem similar to that first

Table III. Values of $\varepsilon_{\max}$ for $\hat{s}G(\hat{s}, k, \varepsilon)$ to be passive.

Value of k	Number of pole-zero pairs allowed N						
	1	2	3	4	5	6	∞
–1.0	∞	0.095	0.095	0.017	0.017	0.006	0
–0.7	∞	0.115	0.115	0.020	0.020	0.008	0
–0.5	∞	0.141	0.141	0.025	0.025	0.010	0
–0.3	∞	0.202	0.202	0.036	0.036	0.014	0
–0.1	∞	0.504	0.504	0.091	0.091	0.037	0
–0.0	∞	∞	∞	∞	∞	∞	∞
+0.1	2.491	2.491	0.147	0.147	0.045	0.045	0
+0.3	0.612	0.612	0.039	0.039	0.011	0.011	0
+0.5	0.232	0.232	0.017	0.017	0.005	0.005	0
+0.7	0.063	0.063	0.008	0.008	0.002	0.002	0
+0.73	0.044	0.044	0.007	0.007	0.002	0.002	0

Example: For $k=-1$, $\hat{s}G(\hat{s}, k, \varepsilon)$ is passive admitting 3 pole-zero pairs on the positive imaginary axis if $0.017<\varepsilon<0.095$.

https://doi.org/10.1017/S0263574702004538 Published online by Cambridge University Press

https://doi.org/10.1017/S0263574702004538 Published online by Cambridge University Press

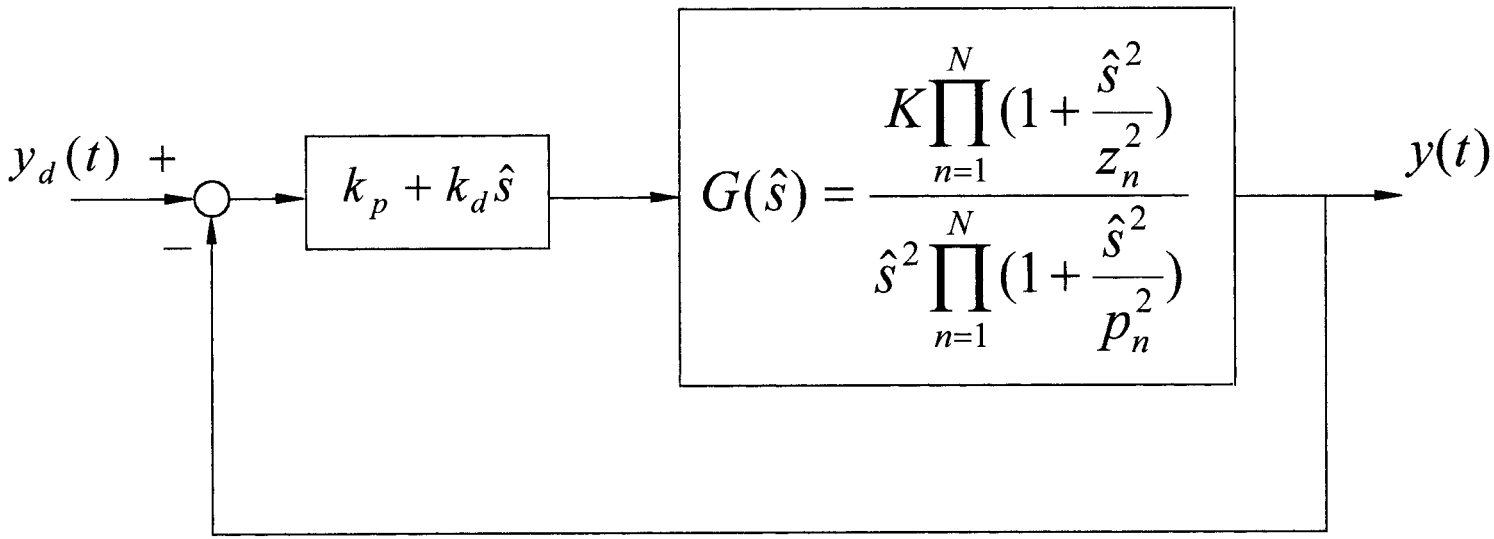


Fig. 4. Passivity-based PD control structure.

established by Gevarter[15] for collocated truncated transfer function but readily applicable to the noncollocated truncated passive transfer functions $\hat{s}G(\hat{s}, k, \varepsilon)$ is stated below.

Theorem 1: If $\hat{s}G(\hat{s})$ is passive, where $\hat{s}G(\hat{s})$ is in the form of equation (20), then $G(\hat{s})$ is a asymptotically stabilizable by a PD controller. It holds for any finite positive integer N.

Proof: The closed-loop poles of the system shown in Figure 4 are the roots of the characteristic equation

$$(k_p + k_d\hat{s}) \cdot \frac{\prod_{n=1}^{N}\left(1+\frac{\hat{s}^2}{z_n^2}\right)}{\hat{s}^2\prod_{n=1}^{N}\left(1+\frac{\hat{s}^2}{p_n^2}\right)} = -1, \tag{21}$$

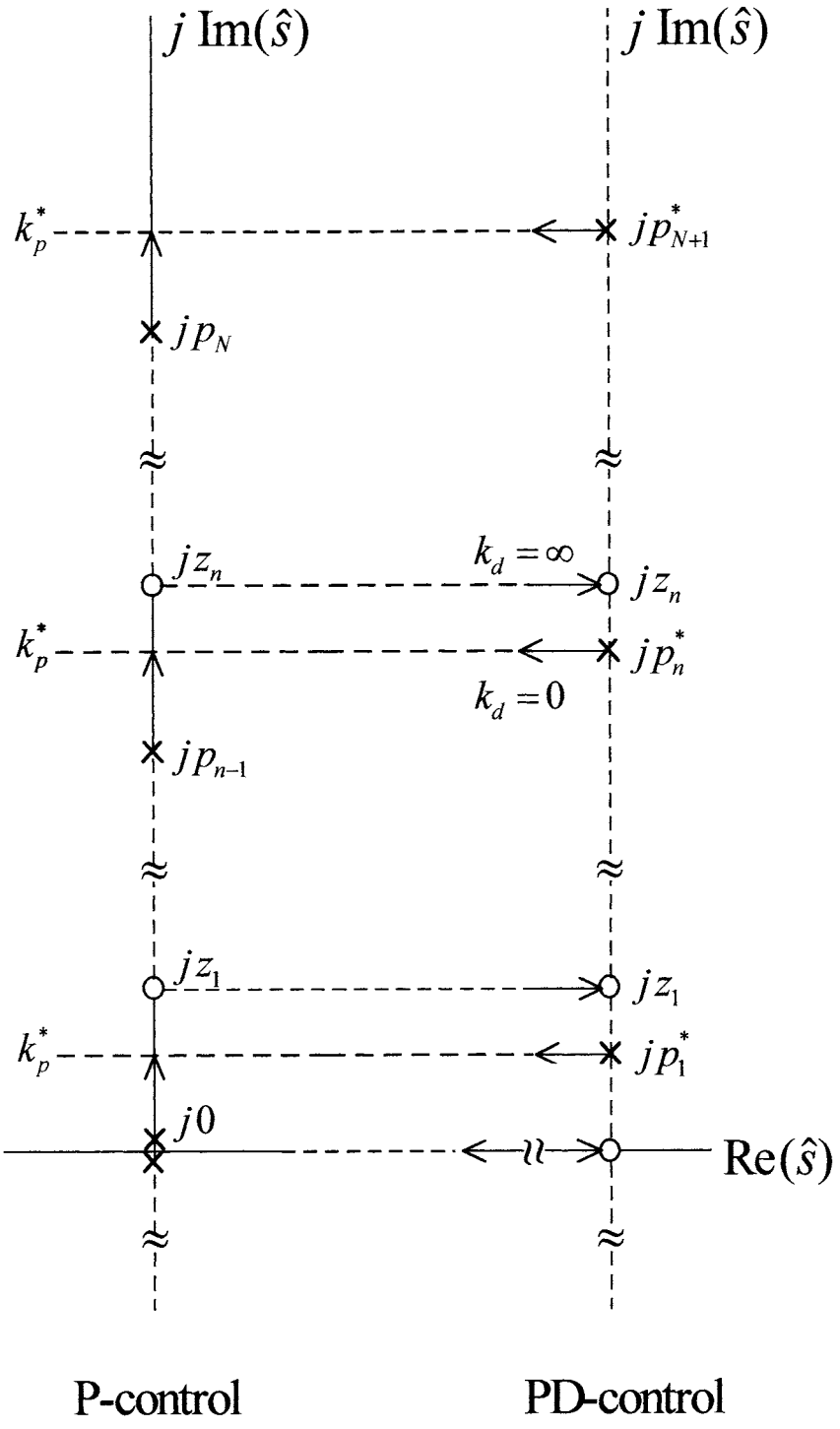


Fig. 5. Root locus of equation (21).

https://doi.org/10.1017/S0263574702004538 Published online by Cambridge University Press

in which $p_{n-1}<z_n<p_n$, $p_0=0$, $n=1, 2, \cdots, N$ due to the passivity property of $\hat{s}G(\hat{s})$. Clearly, with $k_d=0$, the effect of P-control alone is merely to move all the closed-loop poles along the imaginary $\hat{s}$-axis from $\hat{s}=\pm jp_{n-1}$ to $\hat{s}=\pm jz_n$, $n=1, 2, \cdots, N+1$, $z_{N+1}=\infty$ as k_p changes from 0 to ∞ (see Figure 5). Let the roots of equation (21) corresponding to $k_d=0$ and $k_p=k_p^*$ be $\hat{s}=\pm jp_n^*$, where $p_{n-1}<p_n^*<z_n$, $n=1, 2, \cdots, N+1$, $z_{N+1}=\infty$. Equation (21) can now be written as

$$\frac{k_d}{k_p^*}\cdot\frac{\hat{s}\prod_{n=1}^{N}\left(1+\frac{\hat{s}^2}{z_n^2}\right)}{\prod_{n=1}^{N+1}\left(1+\frac{\hat{s}^2}{p_n^{*2}}\right)}=-1. \tag{22}$$

Because of the $\pm 180°$ phase angle requirement, the roots of equation (22) on the imaginary $\hat{s}$-axis are restricted only to the points $\hat{s}=\pm jp_n^*$, $n=1, 2, \cdots, N+1$ and $\hat{s}=0$, $\pm jz_n$, $n=1, 2, \cdots, N$. The angles of departures from $\hat{s}=\pm jp_n^*$, $n=1, 2, \cdots, N+1$ and the angle of arrivals at $\hat{s}=0$, $\pm jz_n$, $n=1, 2, \cdots, N$ are all $\pm 180°$ with respect to the positive real $\hat{s}$-axis (see Figure 5). Since one of the zeros is at infinity, a branch of the root loci extends to infinity along the negative real axis (the asymptote). Therefore, the root loci stay in the open left half-plane for all $0<k_p<\infty$, $0<k_d<\infty$ since they cannot cross the imaginary $\hat{s}$-axis. This concludes the proof. □

Consider the noncollocated truncated transfer function $G_1(\hat{s}, k, \varepsilon_1)$ as shown in Figure 6 such that $\hat{s}G_1(\hat{s}, k, \varepsilon_1)$ is passive. With the PD control law

$$\tau_1(\hat{s})=-(k_{p1}+k_{d1}\hat{s})\cdot[y_1(\hat{s}, k, \varepsilon_1)-y_d(\hat{s})], \tag{23}$$

where $y_d(\hat{s})$ is the Laplace transform of the desired output trajectory, then

$$y_1(\hat{s}, k, \varepsilon_1)=\frac{(k_{p1}+k_{d1}\hat{s})\cdot G_1(\hat{s}, k, \varepsilon_1)}{1+(k_{p1}+k_{d1}\hat{s})\cdot G_1(\hat{s}, k, \varepsilon_1)}\,y_d(\hat{s}). \tag{24}$$

From equations (23) and (24), $\tau_1(\hat{s})$ can further be expressed as

$$\tau_1(\hat{s})=\frac{k_{p1}+k_{d1}\hat{s}}{1+(k_{p1}+k_{d1}\hat{s})\cdot G_1(\hat{s}, k, \varepsilon_1)}\,y_d(\hat{s}). \tag{25}$$

The closed-loop responses of the tip position $w(\ell, t)=y_1(t, 1, \varepsilon_1)$ and the hub angular position $\ell\theta(t)=y_1(t, 0, \varepsilon_1)$ are given, respectively, by

$$y_1(\hat{s}, 1, \varepsilon_1)=G_1(\hat{s}, 1, \varepsilon_1)\tau_1(\hat{s}), \quad y_1(\hat{s}, 0, \varepsilon_1)=G_1(\hat{s}, 0, \varepsilon_1)\tau_1(\hat{s}). \tag{26}$$

The time functions $\tau_1(t)$, $y_1(t, 1, \varepsilon_1)$ and $y_1(t, 0, \varepsilon_1)$ can then be calculated by taking the inverse Laplace transform of equations (25) and (26). With G_1 given by equation (20), it can be easily shown that $\lim_{t\to\infty}(t, k, \varepsilon_1)=\lim_{t\to\infty}y_1(t, 1, \varepsilon_1)=\lim_{t\to\infty}y_1(t, 0, \varepsilon_1)=\lim_{s\to 0}sy_d(s)$ provided the limits exist.

3.2. Achieving passivity using root strain feedback

The objective here is to propose a method to render a non-passive truncated transfer function into a passive one by using the root strain feedback. For the system shown in Figure 7, the following is true:

Theorem 2: Let $G_1(\hat{s}, k, \varepsilon_1)$ and $G_2(\hat{s}, k, \varepsilon_2)$ be marginal minimum phase in the form of equation (20). Suppose

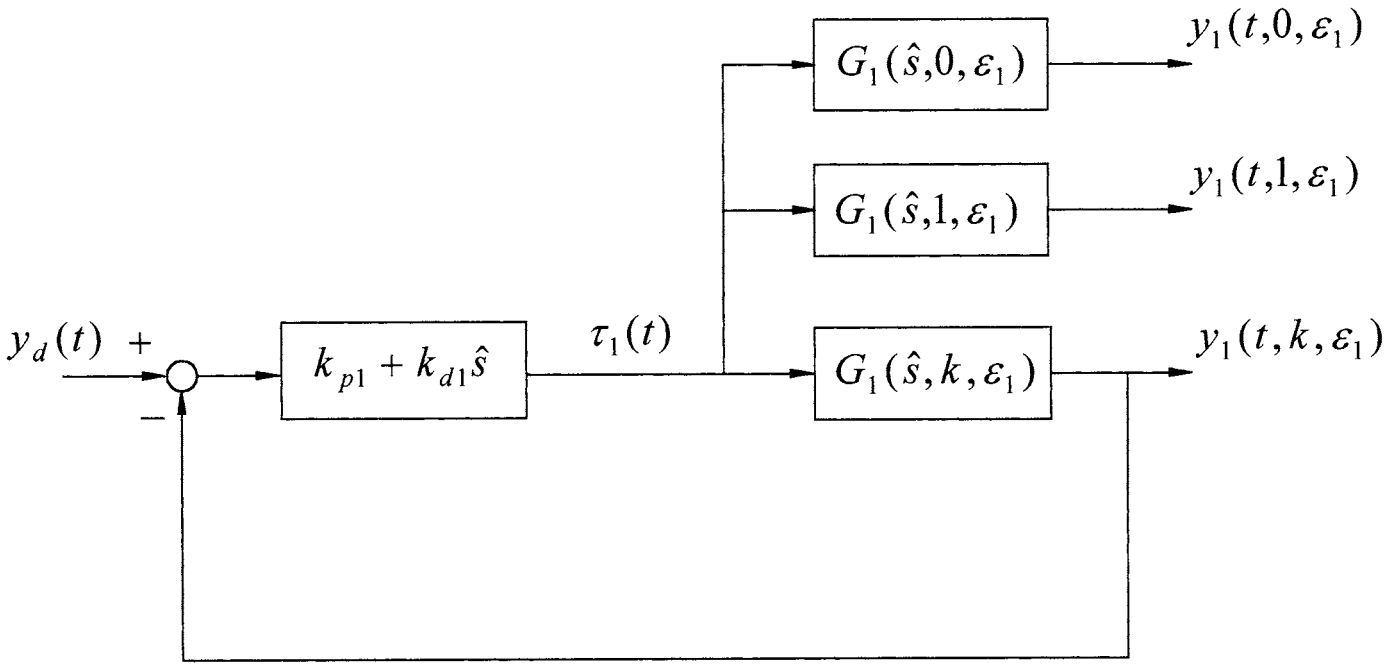


Fig. 6. PD control of a passive $\hat{s}G_1(\hat{s}, k, \varepsilon_1)$: $y_1(t, k, \varepsilon_1)$ is the defined output, $y_1(t, 1, \varepsilon_1)=w(\ell, t)$ is the tip position, and $y_1(t, 0, \varepsilon_1)=\ell\theta(t)$ is the joint angular position.

https://doi.org/10.1017/S0263574702004538 Published online by Cambridge University Press

https://doi.org/10.1017/S0263574702004538 Published online by Cambridge University Press

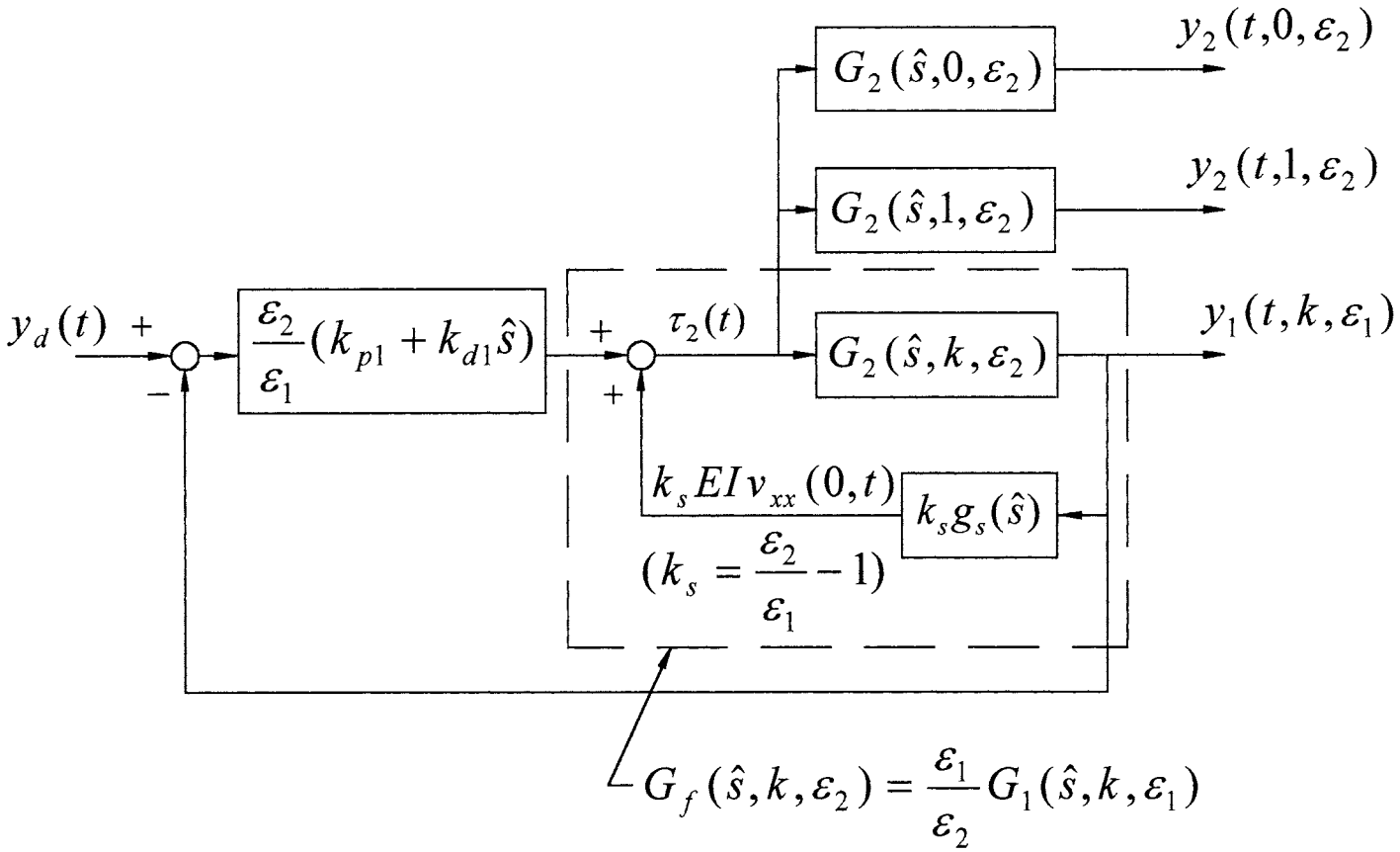


Fig. 7. Passivation of $G_2(\hat{s}, k, \varepsilon_2)$ by root-strain feedback.

$\hat{s}G_2(\hat{s}, k, \varepsilon_2)$ is not passive but $\hat{s}G_1(\hat{s}, k, \varepsilon_1)$ is passive. Assume further that $k<0.758$ and $\varepsilon_2>\varepsilon_1>0$. Then there exists a root strain feedback $u(t)=k_s EIv_{xx}(0, t)$, when it is applied to $G_2(\hat{s}, k, \varepsilon_2)$, that will transform $G_2(\hat{s}, k, \varepsilon_2)$ into $\frac{\varepsilon_1}{\varepsilon_2} G_1(\hat{s}, k, \varepsilon_1)$, where $k_s=\frac{\varepsilon_2}{\varepsilon_1}-1$. Using the PD controller shown in Figure 7, the closed-loop system achieves the same performance as that of Figure 6. Specifically, $y_2(t, k, \varepsilon_2)=y_1(t, k, \varepsilon_1)$, $y_2(t, 1, \varepsilon_2)=y_1(t, 1, \varepsilon_1)$ and $y_2(t, 0, \varepsilon_2)=y_1(t, 0, \varepsilon_1)$.

Proof: From equations (9), (12) and (15), the open-loop transfer functions G_1 and G_2 can be expressed as

$$G_1(\hat{s}, k, \varepsilon_1)=\frac{3\ell^2}{EI}\cdot\frac{\prod_{n=1}^{N}\left(1+\frac{\hat{s}^2}{\omega_{\alpha n}^2}\right)}{\hat{s}^2\left[\prod_{n=1}^{N}\left(1+\frac{\hat{s}^2}{\omega_{\beta n}^2}\right)+3\varepsilon_1\prod_{n=1}^{N}\left(1+\frac{\hat{s}^2}{\omega_{pn}^2}\right)\right]} \tag{27}$$

and

$$G_2(\hat{s}, k, \varepsilon_2)=\frac{3\ell^2}{EI}\cdot\frac{\prod_{n=1}^{N}\left(1+\frac{\hat{s}^2}{\omega_{\alpha n}^2}\right)}{\hat{s}^2\left[\prod_{n=1}^{N}\left(1+\frac{\hat{s}^2}{\omega_{\beta n}^2}\right)+3\varepsilon_2\prod_{n=1}^{N}\left(1+\frac{\hat{s}^2}{\omega_{pn}^2}\right)\right]}. \tag{28}$$

With the root strain feedback given by equation (52) in Appendix A, the plant G_2 is transformed into

$$\begin{aligned}G_f(\hat{s}, k, \varepsilon_2)&=\frac{G_2(\hat{s}, k, \varepsilon_2)}{1-k_s g_s(\hat{s})G_2(\hat{s}, k, \varepsilon_2)}\\&=\frac{1}{1+k_s}\cdot\frac{3\ell^2}{EI}\\&\quad\cdot\frac{\prod_{n=1}^{N}\left(1+\frac{\hat{s}^2}{\omega_{\alpha n}^2}\right)}{\hat{s}^2\left[\prod_{n=1}^{N}\left(1+\frac{\hat{s}^2}{\omega_{\beta n}^2}\right)+\frac{3\varepsilon_2}{1+k_s}\prod_{n=1}^{N}\left(1+\frac{\hat{s}^2}{\omega_{pn}^2}\right)\right]}.\end{aligned} \tag{29}$$

Let $\frac{\varepsilon_2}{1+k_s}=\varepsilon_1$, then $k_s=\frac{\varepsilon_2}{\varepsilon_1}-1$. In view of equation (27), equation (29) reduces to

$$G_f(\hat{s}, k, \varepsilon_2)=\frac{\varepsilon_1}{\varepsilon_2} G_1(\hat{s}, k, \varepsilon_1). \tag{30}$$

Using the PD controller shown in Figure 7, it is obvious that $y_2(t, k, \varepsilon_2)=y_1(t, k, \varepsilon_1)$. From Figures 6 and 7, it must be true that

$$\frac{Z_2(\hat{s}, k)}{P_2(\hat{s}, \varepsilon_2)}\tau_2(\hat{s})=\frac{Z_1(\hat{s}, k)}{P_1(\hat{s}, \varepsilon_1)}\tau_1(\hat{s}), \tag{31}$$

$$y_2(\hat{s}, 1, \varepsilon_2)=\frac{Z_2(\hat{s}, 1)}{P_2(\hat{s}, \varepsilon_2)}\tau_2(\hat{s}), \tag{32}$$

$$y_1(\hat{s}, 1, \varepsilon_1)=\frac{Z_1(\hat{s}, 1)}{P_1(\hat{s}, \varepsilon_1)}\tau_1(\hat{s}). \tag{33}$$

It follows immediately that $y_2(t, 1, \varepsilon_2)=y_1(t, 1, \varepsilon_1)$. Similarly, $y_2(t, 0, \varepsilon_2)=y_1(t, 0, \varepsilon_1)$. This completes the proof. □

Note from equation (29) that the effect of root strain feedback is merely to move the poles along the imaginary $\hat{s}$-axis from $\hat{s}=\pm j\omega_{\theta n}(\varepsilon_2)$ to $\hat{s}=\pm j\omega_{\beta n}=\pm j\omega_{\theta n}(\varepsilon_1=0))$ as k_s changes from 0 to ∞ (see Figure 3). A smaller ε_1 implies that a passive truncated transfer function admitting more higher order flexible modes can be obtained via the root strain feedback (see Table III). The realization of this approach can be accomplished by measuring the root strain using strain gauges rather than the reconstruction of $v_{xx}(0, t)$ from $y_1(t, k, \varepsilon_1)$.

Following a similar approach, it can be shown that a marginal minimum phase $G_2(\hat{s}, k, \varepsilon_2)$ can be rendered passive by using a root shear force feedback of the form $u(t)=k_f\ell EIv_{xxx}(0, t)$. However, the effect of k_f is to move the poles along the imaginary $\hat{s}$-axis from $\hat{s}=\pm j\omega_{\theta n}(\varepsilon_2)$ to $\hat{s}=\pm jn^2\pi^2$ as k_f changes from 0 to ∞ (use equation (53) in Appendix A). Since this result is less attractive than the root strain feedback, the details are omitted here.

A recent result[25,26] has shown that any controllable linear system is (state) feedback equivalent to a passive system if and only if it has relative degree one and is marginal minimum phase. However, the essence of the above Theorem 2 is to transform a marginal minimum phase linear system of relative degree two into a passive system using only output feedback.

3.3. Achieving passivity using joint angular acceleration feedback

An alternative method of converting a non-passive truncated transfer function into a passive one is to use the feedback of the joint angular acceleration. For the system shown in Figure 8, the following is true:

Theorem 3: Let $G_1(\hat{s}, k, \varepsilon_1)$ and $G_2(\hat{s}, k, \varepsilon_2)$ be marginal minimum phase in the form of equation (20). Suppose $\hat{s}G_2(\hat{s}, k, \varepsilon_2)$ is not passive but $\hat{s}G_1(\hat{s}, k, \varepsilon_1)$ is passive. Assume further that $k<0.758$ and $\varepsilon_2>\varepsilon_1\geq 0$. Then there exists a joint angular acceleration feedback $u(t)=k_a\rho\ell^3\ddot{\theta}(t)$, when it is applied to $G_2(\hat{s}, k, \varepsilon_2)$, that transforms $G_2(\hat{s}, k, \varepsilon_2)$ into $G_1(\hat{s}, k, \varepsilon_1)$, where $k_a=\varepsilon_2-\varepsilon_1$. Using the PD controller shown in Figure 8, the closed-loop system achieves the

https://doi.org/10.1017/S0263574702004538 Published online by Cambridge University Press

https://doi.org/10.1017/S0263574702004538 Published online by Cambridge University Press

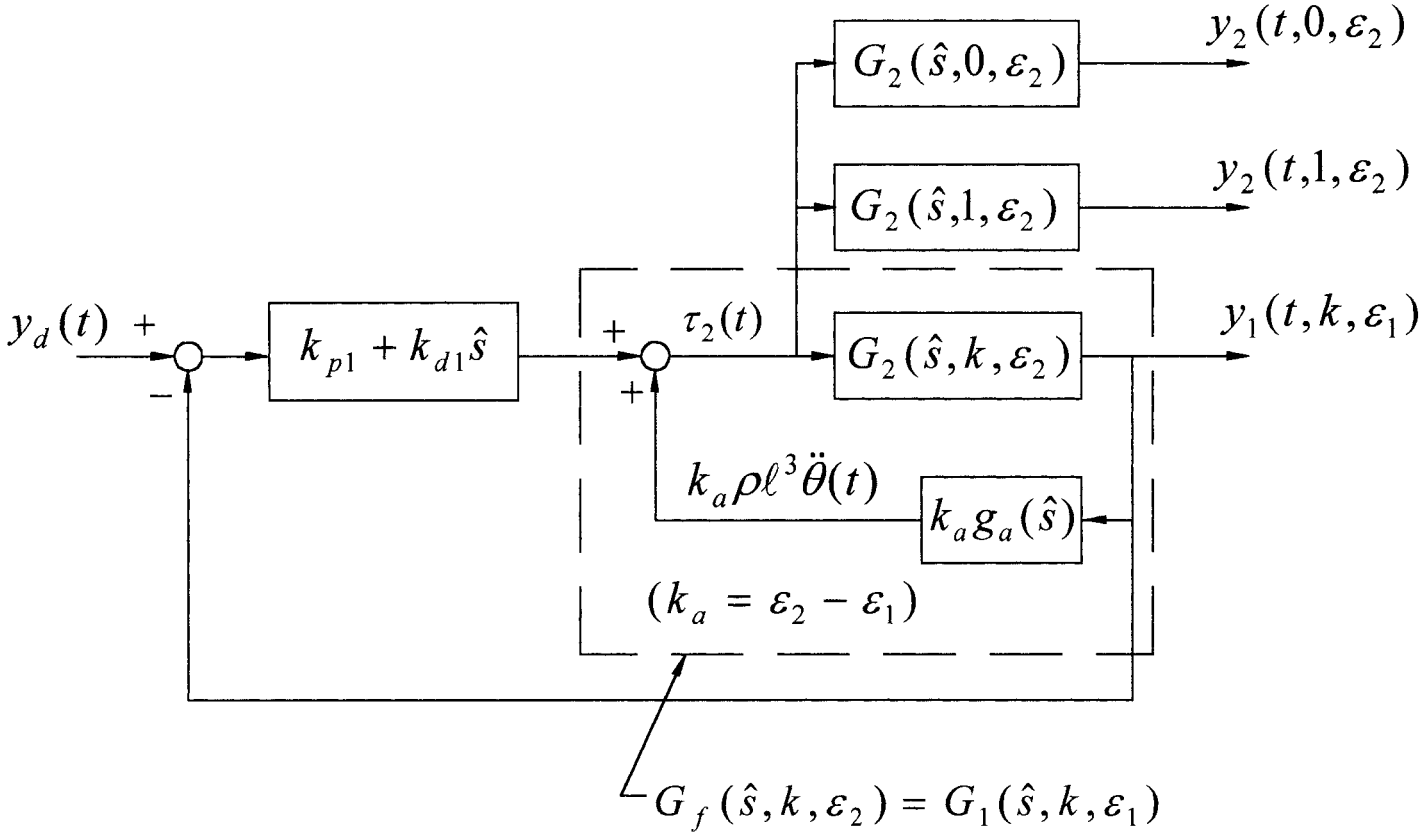


Fig. 8. Passivation of $G_2(\hat{s}, k, \varepsilon_2)$ by joint-angular-acceleration feedback.

same perforrnance as that of Figure 6. Specifically, $y_2(t, k, \varepsilon_2)=y_1(t, k, \varepsilon_1)$, $y_2(t, 1, \varepsilon_2)=y_1(t, 1, \varepsilon_1)$ and $y_2(t, 0, \varepsilon_2)=y_1(t, 0, \varepsilon_1)$.

Proof: With the joint angular acceleration feedback given by equation (54) in Appendix A, the plant G_2 is transformed into

$$G_f(\hat{s}, k, \varepsilon_2)$$

$$=\frac{G_2(\hat{s}, k, \varepsilon_2)}{1-k_a g_a(\hat{s})G_2(\hat{s}, k, \varepsilon_2)}$$

$$=\frac{3\ell^2}{EI}\cdot\frac{\prod_{n=1}^{N}\left(1+\frac{\hat{s}^2}{\omega_{\alpha n}^2}\right)}{\hat{s}^2\left[\prod_{n=1}^{N}\left(1+\frac{\hat{s}^2}{\omega_{\beta n}^2}\right)+3(\varepsilon_2-k_a)\prod_{n=1}^{N}\left(1+\frac{\hat{s}^2}{\omega_{pn}^2}\right)\right]}. \tag{34}$$

Letting $k_a=\varepsilon_2-\varepsilon_1$, and using equation (27), equation (34) reduces to

$$G_f(\hat{s}, k, \varepsilon_2)=G_1(\hat{s}, k, \varepsilon_1). \tag{35}$$

The rest of the proof is essentially the same as in Theorem 2. □

Note from equation (34) that the effect of the joint angular acceleration feedback is to move the poles along the imaginary $\hat{s}$-axis from $\hat{s}=\pm j\omega_{\theta n}(\varepsilon_2)$ to $\hat{s}=\pm j\omega_{\beta n}=\pm j\omega_{\theta n}(\varepsilon_1=0)$ as k_a changes from 0 to ε_2. Thus, an infinitedimensional passive transfer function can be recovered if $k_a=\varepsilon_2$. With the current development of rotary acceleration sensor,[27] the realization of this approach is worthy of every endeavor.

Suppose a tip acceleration feedback of the form $u(t)=k_t\rho\ell^2\ddot{w}(\ell, t)$ is considered. The effect of the tip acceleration feedback is found to move the poles along the imaginary $\hat{s}$-axis from $\hat{s}=\pm j\omega_{\theta n}(\varepsilon_2)$ to the real zeros $\hat{s}=\pm\omega_{zn}$ as k_t changes from 0 to ∞ (use equation (55) in Appendix A). Thus, the passivation through the use of tip acceleration feedback is difficult if not impossible. The details are omitted.

4. SIMULATION RESULTS

The effectiveness of the proposed control approaches is evaluated here through numerical simulations using the parameters of an experimental apparatus given in Tokhi and Azad.[28] These parameters are: $I_{h1}=5.86\times10^{-4}$ kg − m^2, $\ell=0.96$ m, $\rho=0.1649$ kg/m, $E=7\times10^{10}$ N/m^2 and $I=5.1924\times10^{-11}$ m^4.

4.1. Control of truncated passive transfer functions

As an application of Theorem 1, the performance of the collocated ($k=0$) and noncollocated ($k=0.7$ and -1) PD control of the aforementioned single-link flexible manipulator are compared. Note that $k=0.7$ is close to the tip ($k=1$), but it is still away from the possible pole-zero cancellation region occurring when $0.730\le k<0.758$ (see Figure 3). Since $\varepsilon_1=\frac{I_{h1}}{\rho\ell^3}=0.004$, it can be seen from Table III that the transfer function

$$\hat{s}G_1(\hat{s}, k, \varepsilon_1)=\frac{3\ell^2}{(1+3\varepsilon_1)EI}\cdot\frac{\prod_{n=1}^{4}\left(1+\frac{\hat{s}^2}{\omega_{\alpha n}^2}\right)}{\hat{s}\prod_{n=1}^{4}\left(1+\frac{\hat{s}^2}{\omega_{\theta n}^2}\right)} \tag{36}$$

is passive for all $k=0.7$, 0, and -1. The first four pairs of nonzero poles are found to be $\hat{s}=\pm j\omega_{\theta n}=\pm3.810^2j$, $\pm6.283^2j$, $\pm8.463^2j$ and $\pm11.207^2j$. The first four pairs of zeros $\hat{s}=\pm j\omega_{\alpha n}$ for $k=0.7$, 0 and -1 are given in Table II. For each specific value of k the values of k_{p1} and k_{d1} are selected based on several root locus plots of the denominator of equation (24) such that the negative real closed-loop poles are far away from the imaginary $\hat{s}$-axis. The resulting controller gains are as follows: (a) $k_{p1}=13.317$, $k_{d1}=7.682$ for $k=0.7$, (b) $k_{p1}=2.204$, $k_{d1}=3.318$ for $k=0$, and (c) $k_{p1}=0.996$, $k_{d1}=2.114$ for $k=-1$. Let the desired output trajectory be $y_d(t)=1-9e^{-8t}+8e^{-9t}$. The tip position $w_1(\ell, t)$ and driving toque $\tau_1(\ell)$ can be computed using equations (26) and (25) for $k=0.7$, 0, and -1. The simulation results are shown in Figures 9 and 10. As expected, the response of the tip position based on a noncollocated output closest to the tips (i.e., $k=0.7$) is much better than the others, but at the expense of a larger peak torque.

4.2. Control of a truncated non-passive minimum phase transfer function

If the hub inertia in the above example is increased by 100 times, then $\varepsilon_2=0.4$. It can be seen from Table III that the truncated transfer functions corresponding to $k=0.7$ and -1 are passive only for $N=0$ and $N=1$, respectively. Wlth the application of Theorem 2 or Theorem 3, the same performance as that of $\varepsilon_2=0.004$ can be achieved by using a root strain feedback ($k_s=99$) or a joint angular acceleration feedback ($k_a=0.396$). The driving torque $\tau_2(t)$, which is different from $\tau_1(t)$, can be calculated using equation (31). As shown in Figure 11, for the case $k=0.7$, the same performance is achieved at the cost of a larger peak torque. Of course, an alternative strictly passive compensator other than the PD controller can be designed for the feedback passive transfer function $\hat{s}G_f(\hat{s}, k, \varepsilon_2)$.

5. CONCLUSIONS

In this work, the passivity property of a noncollocated single-link flexible manipulator without a tip payload has been investigated. The torque applied to the joint is taken as the input, and the joint angle plus a weighted value of tip deflection is considered as the output. The weighting factor k of the tip deflection and a measure ε of the hub-to-beam

https://doi.org/10.1017/S0263574702004538 Published online by Cambridge University Press

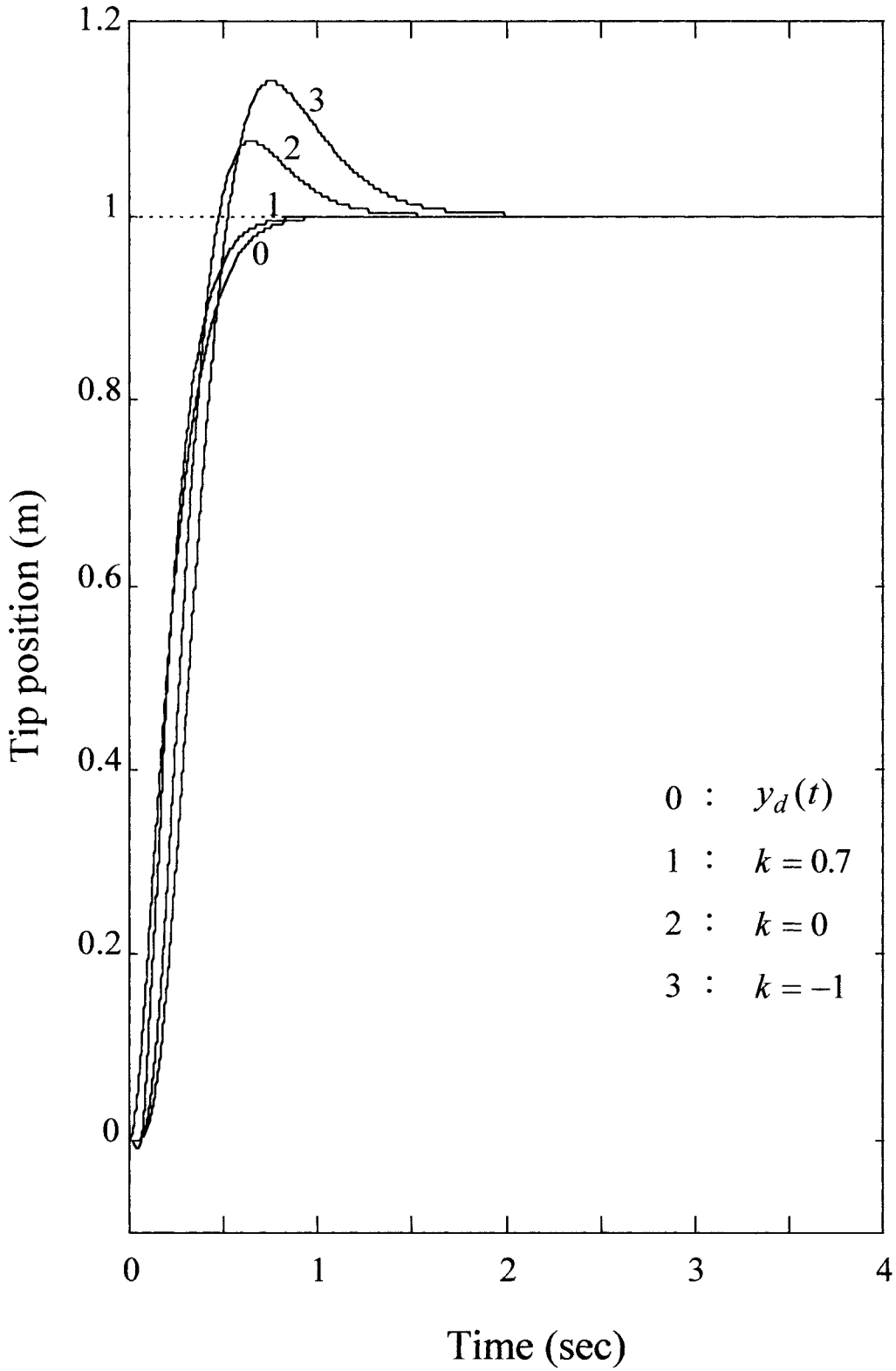


Fig. 9. Tip position $y_1(t, 1, \varepsilon_1)$ for $\varepsilon_1 = 0.004$ and $k = 0.7, 0, -1$.

inertia ratio are the two parameters of vital importance. For a linear infinite dimensional model of the single-link flexible system, its irrational transfer function can be represented by an infinite product expression. This irrational transfer function is passive if either (a) $k=0$, $0 \le \varepsilon < \infty$ or (b) $\varepsilon = 0$, $-\infty < k < 0.730$ is satisfied. In the general case, passivity can be achieved only for a truncated transfer function. The number of flexible modes admitted in a truncated passive transfer function depends on the values of k and ε. To include higher order flexible modes would require the adjustment of k and ε to their respective smaller absolute values.

On the other hand, it has also been proved in this work that a non-passive, marginal minimum-phase truncated transfer function can be rendered passive by the feedback of either root-strain or joint-angular-acceleration. Any number

https://doi.org/10.1017/S0263574702004538 Published online by Cambridge University Press

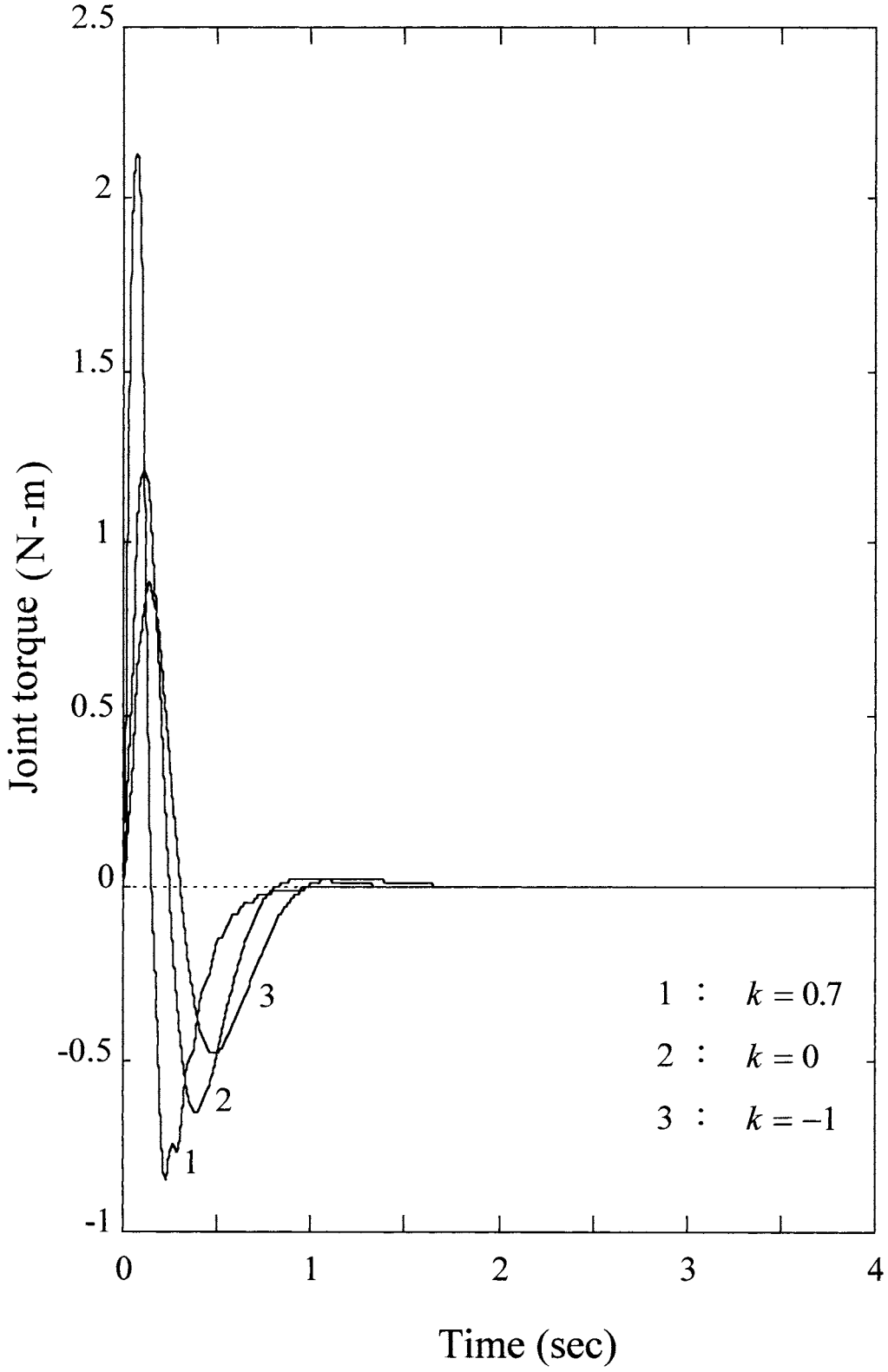


Fig. 10. Control torque $\tau_1(t)$ for $\varepsilon_1=0.004$ and $k=0.7, 0, -1$.

of flexible modes can be included in the feedback passive transfer function by adjusting the feedback gains. The important role played by the root-strain feedback or the joint angular acceleration feedback in achieving passivity has apparently not been previously reported on in the literature.

For the noncollocated passive truncated transfer function, it has been shown that a feedforward PD controller ensures a desired output step response to be asymptotically tracked by the defined output as well as the actual tip point of the flexible link. Numerical simulations have demonstrated the achievable performance based on the aforementioned controller design concepts.

Some boundary control strategies based on the original linear infinite-dimensional model have been proposed[29–31] for the link-vibration suppression, regulation and orientation of the rigid hub. The extension of these results to the

https://doi.org/10.1017/S0263574702004538 Published online by Cambridge University Press

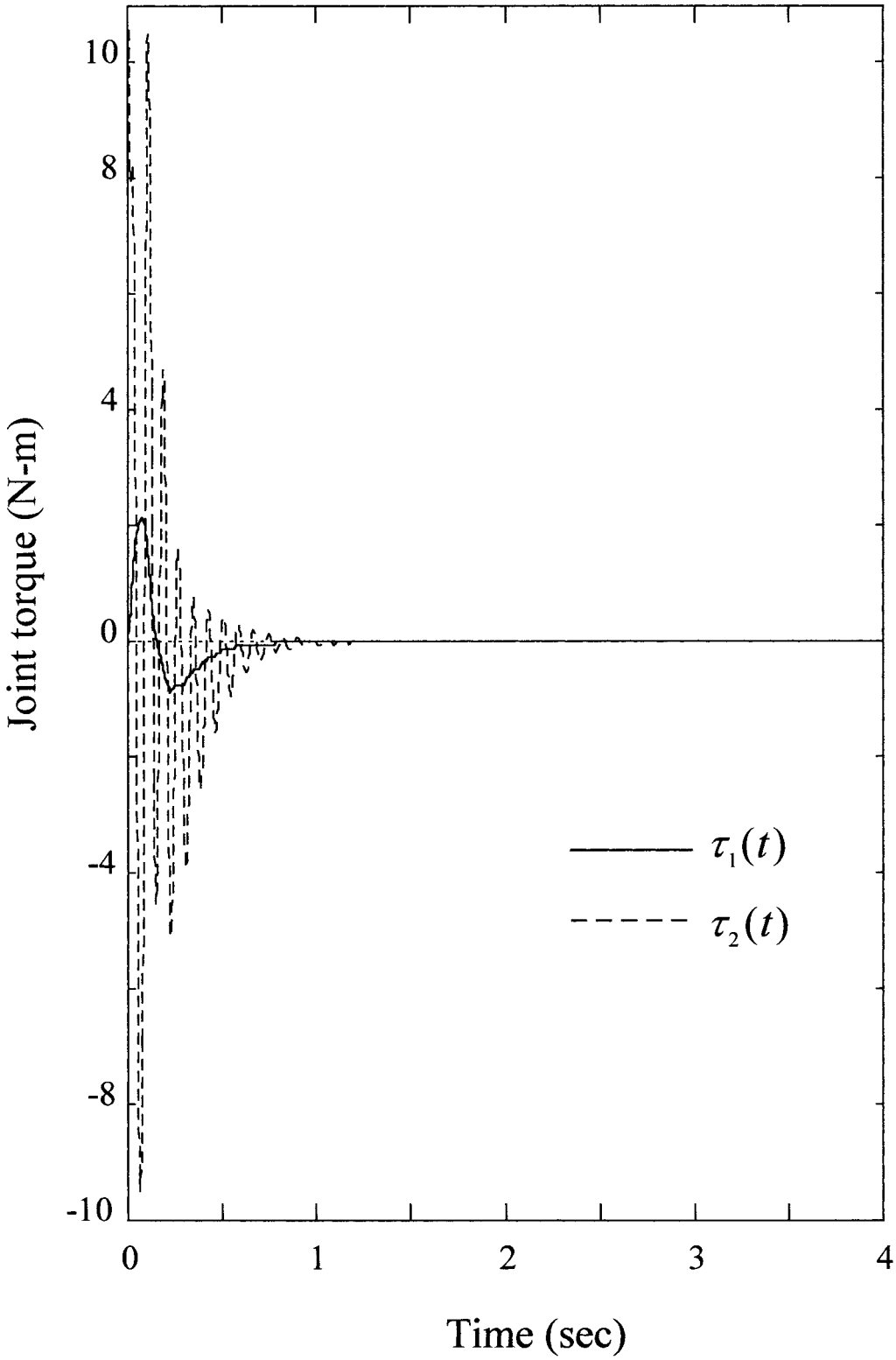


Fig. 11. Comparison of control torques.

problem of link-tip trajectory tracking using only the joint torque is important and remains a challenging one.

References

1. R.H. Cannon and E. Schmitz, "Initial Experiments on the Control a Flexible Manipulator," *Int. J. of Rob. Res.* **3**, 62–75 (1984).
2. V.A. Spector and H. Flashner, "Modeling and Design Implications of Noncollocated Control in Flexible Systems," *ASME J. of Dyn. Sys. Meas. And Contr.* **112**, 186–193 (1990).
3. J.H. Park and H. Asada, "Dynamic Analysis of Noncollocated Flexible Arms and Design of Torque Transmission Mechanism," *ASME J. of Dyn. Sys. Meas. And Contr.* **116**, 201–207 (1994).

https://doi.org/10.1017/S0263574702004538 Published online by Cambridge University Press

4. A. De Luca and L. Lanari, "Achieving Minimum Phase Behavior in a One-Link Flexible Arm," *Proc. Int. Symp. on Intelligent Robotics*, Bangalore, India (1991) pp. 325–344.
5. A. De Luca, P. Lucibello and G. Ulivi, "Inversion Techniques for Trajectory Control of Flexible Robot Arms," *J. of Rob. Syst.* **6**, 325–344 (1989).
6. A. De Luca, "Zero Dynamics in Robotics," **In:** *Nonlinear Synthesis* (C. I. Byrnes and A. Kurzhansky, Eds.) (Birkhauser, Boston, 1991) pp. 68–87.
7. S.K. Madhavan and S.N. Singh, "Inverse Trajectory control and Zero Dynamics Sensitivity of an Elastic Manipulator," *Proc. 1991 Amer. Contr. Conf.*, Boston, MA (1991) pp. 1879–1884.
8. D. Wang and M. Vidyasagar, "Transfer Function for a Single-Flexible-Link," *Int. J. Rob. Res.* **10**, 540–549 (1991).
9. T.J. Tarn, C. Guo and A.K. Bejczy, "Issues in the Zeros of Flexible Robot Systems," *Proc. 32nd Allerton Conf. on Communication, Control and Computing* (1994) pp. 641–650.
10. P.A. Chodavarapu and M.W. Spong, "On Noncollocated Control of a Single Flexible Link," *Proc. IEEE Int. Conf. on Rob. Autom.*, Minneapolis, Minnesota (1996) pp. 1101–1106.
11. K. Yuan and L.Y. Liu, "Achieving Minimum Phase Transfer Function for a Noncollocated Single-Link Flexible Manipulator," *Asian J. of Control* **2**, 179–191 (2000).
12. D. Wang and M. Vidyasagar, "Passive Control of a Stiff Flexible Link," *Int. J. of Rob. Res.* **11**, 572–578 (1992).
13. C.A. Desoer and M. Vidyasagar, *Feedback System: Input-Output Properties* (Academic Press, New York, 1975).
14. N. Balabanian and T. Bickart, *Electrical Network Theory* (John Wiley and Sons Inc., New York, 1969).
15. W. Gevarter, "Basic Relation for Control of Flexible Vehicles," *AIAA J.* **8**, 666–672 (1970).
16. E. Barbieri, "Single-Input/Single-Output Transfer Functions for a Flexible Slewing Link," *J. of Rob. Syst.* **10**, 913–929 (1993).
17. R.E. Goodson, "Distributed System Sirnulation Using Infinite Product Expansions," *Simulation*, 255–263 (1970).
18. H. Jeffreys and B.S. Jeffreys, *Method of Mathematical Physics* (2nd edition, Cambridge Univ, Press, 1950).
19. A.G. Chassiakos and G.A. Bekey, "On the Modeling and Control of a Flexible Manipulator Arrn by Point Actuators," *Proc. of 25th Conf. on Decision and Control*, Athens, Greece (1986) pp. 1145–1150.
20. A. De Luca and B. Siciliano, "Inversion-Based Nonlinear Control of Robot Arms with Flexible Links," *J. of Guid. Contr. And Dyn.* **16**, 1169-1176 (1993).
21. M. Rossi, K. Zuo and D. Wang, "Issues in the Design of Passive Controllers for Flexible Link Robots," *Proc. 1994 IEEE Int. Conf. on Rob. Autom.*, San Diego, CA (1994) pp. 321–326.
22. R. Lozano, B. Brogliato, O. Egeland and B. Maschke, *Dissipative Systems Analysis and Control: Theory and Application* (Springer-Verlag, London, 2000).
23. H.R. Pota and M. Vidyasagar, "Passivity of Flexible Beam Transfer Functions with Modified Outputs," *Proc. 1991 IEEE Int. Conf. on Rob. Autom.*, Sacrarnento, CA (1991) pp. 2826–2831.
24. M.E. Rossi and D.W.L. Wang, "Hybrid Passive/Adaptive Control of a Single Flexible Link Manipulator with a Payload," *Proc. 1996 IEEE Int. Conf on Rob. Autom.*, Minneapolis, Minnesota (1996) pp. 2109–2116.
25. A. Saberi, P.V. Kokotovic and H.J. Sussmann, "Global Stabilization of Partially Linear Composite Systems," *SIAM J. Control and Optimization* **28**, 1491–1503 (1990).
26. C.I. Byrnes, A. Isidori and J.C. Willems, "Passivity, Feedback Equivalence, and the Global Stabilization of Minimum Phase Nonlinear Systems," *IEEE Trans. on Automatic Control* **36**, 1228–1240 (1991).
27. I. Godler, A. Akahane, K. Ohnishi and T. Yamashita, "A Novel Rotary Acceleration Sensor," *IEEE Control Systems Magazine*, 56–60 (1995).
28. M.O. Tokbi and A.K.M. Azad, "Modeling of a Single-Link Manipulator System: Theoretical and Practical Investigations," *Robotica* **14**, Part 1, 91–102 (1996).
29. Y. Sakawa, "Feedback Control of Second Order Evolution Equation with Damping," *SIAM J. Contr. and Opt.* **22**, 343–361 (1984).
30. Z.H. Luo, "Direct Strain Feedback Control of Flexible Robot Arms: New Theoretical and Experimental Results," *IEEE Trans, on Automatic Control* **38**, 1610–1622 (1993).
31. Z.H. Luo and B.Z. Guo, "Shear Forces Feedback of a Single-Link Flexible Robot with a Revolute Joint," *IEEE Trans. on Automatic Control* **42**, 53–65 (1997).

APPENDIX A

By using the definitions of s, β and $\hat{s}$ given in equation (8), the zero-state solution of equation (2) can be written as

$$w(x, s)=C_1 \cosh \frac{\beta}{\ell} x+C_2 \cos \frac{\beta}{\ell} x+C_3 \sinh \frac{\beta}{\ell} x+C_4 \sin \frac{\beta}{\ell} x. \tag{37}$$

The substitution of equation (37) into equations (3)–(5) yields five equations involving C_1, C_2, C_3, C_4, θ, and τ. One obtains

$$C_2=-C_1, \tag{38}$$

$$C_3=-C_1(1+\cosh \beta \cos \beta-\sin \beta \sinh \beta)\,\Delta^{-1}, \tag{39}$$

$$C_4=-C_1(1+\cosh \beta \cos \beta+\sin \beta \sinh \beta)\,\Delta^{-1}, \tag{40}$$

$$\theta(\hat{s})=-2C_1 \frac{\beta}{\ell}(1+\cosh \beta \cos \beta)\,\Delta^{-1}, \tag{41}$$

$$\tau(\hat{s})=-2C_1 \frac{EI}{\ell^2}\beta[\beta(\sinh \beta \cos \beta-\sin \beta \cosh \beta) + \varepsilon \hat{s}^2(1+\cosh \beta \cos \beta)]\,\Delta^{-1}, \tag{42}$$

where

$$\Delta(\hat{s})=\sinh \beta \cos \beta-\sin \beta \cosh \beta. \tag{43}$$

Using equations (37), (1) and (6), one further obtains

$$w(\ell, \hat{s})=-2C_1(\sin \beta+\sinh \beta)\,\Delta^{-1}, \tag{44}$$

$$v(\ell, \hat{s})=-2C_1\beta[(\sin \beta+\sinh \beta)\beta^{-1} - (1+\cosh \beta \cos \beta)]\,\Delta^{-1}, \tag{45}$$

$$y(\hat{s})=-2C_1\beta[(1-k)(1+\cosh \beta \cos \beta) + k(\sin \beta+\sinh \beta)\beta^{-1}]\,\Delta^{-1}, \tag{46}$$

$$v_{xx}(0, \hat{s})=w_{xx}(0, \hat{s})=2C_1 \frac{\beta^2}{\ell^2}, \tag{47}$$

$$v_{xxx}(0, \hat{s})=w_{xxx}(0, \hat{s})=2C_1 \frac{\beta^3}{\ell^3} \sin \beta \sinh \beta\,\Delta^{-1}. \tag{48}$$

Therefore,

$$G(\hat{s}, k, \varepsilon):=\frac{y(\hat{s})}{\tau(\hat{s})}=\frac{\ell^2}{EI} \cdot \frac{(1-k)(1+\cosh \beta \cos \beta)+k\beta^{-1}(\sinh \beta+\sin \beta)}{\beta(\sinh \beta \cos \beta-\cosh \beta \sin \beta)-\varepsilon\beta^4(1+\cosh \beta \cos \beta)}. \tag{49}$$

https://doi.org/10.1017/S0263574702004538 Published online by Cambridge University Press

It has been shown in Section 2.1 that

$$(1-k)(1+\cosh\beta\cos\beta)+k\beta^{-1}(\sinh\beta+\sin\beta)$$

$$=2\prod_{n=1}^{\infty}\left(1+\frac{\hat{s}^2}{\omega_{\alpha n}^2}\right) \text{ for } k\le 0.758, \tag{50}$$

$$\beta(\sinh\beta\cos\beta-\cosh\beta\sin\beta)-\varepsilon\beta^4(1+\cosh\beta\cos\beta)$$

$$=\frac{2}{3}(1+3\varepsilon)\hat{s}^2\prod_{n=1}^{\infty}\left(1+\frac{\hat{s}^2}{\omega_{\theta n}^2}\right) \text{ for } \varepsilon\ge 0. \tag{51}$$

Using the infinite product expansions given in Appendix B, the following transfer functions can also be obtained for $k\le 0.758$:

$$g_s(\hat{s}):=\frac{EIv_{xx}(0,\hat{s})}{y(\hat{s})}=-\frac{EI}{3\ell^2}\cdot\frac{\hat{s}^2\prod_{n=1}^{N}\left(1+\frac{\hat{s}^2}{\omega_{\beta n}^2}\right)}{\prod_{n=1}^{N}\left(1+\frac{\hat{s}^2}{\omega_{\alpha n}^2}\right)},\qquad N\to\infty, \tag{52}$$

$$g_f(\hat{s}):=\frac{EI\ell v_{xxx}(0,\hat{s})}{y(\hat{s})}=\frac{EI}{2\ell^2}\cdot\frac{\hat{s}^2\prod_{n=1}^{N}\left(1+\frac{\hat{s}^2}{n^4\pi^4}\right)}{\prod_{n=1}^{N}\left(1+\frac{\hat{s}^2}{\omega_{\alpha n}^2}\right)},\qquad N\to\infty, \tag{53}$$

$$g_a(\hat{s}):=\frac{\rho\ell^3 s^2\theta(\hat{s})}{y(\hat{s})}=\frac{EI}{\ell^2}\cdot\frac{\hat{s}^2\prod_{n=1}^{N}\left(1+\frac{\hat{s}^2}{\omega_{pn}^2}\right)}{\prod_{n=1}^{N}\left(1+\frac{\hat{s}^2}{\omega_{\alpha n}^2}\right)},\qquad N\to\infty, \tag{54}$$

$$g_t(\hat{s}):=\frac{\rho\ell^2 s^2 w(\ell,\hat{s})}{y(\hat{s})}=\frac{EI}{\ell^2}\cdot\frac{\hat{s}^2\prod_{n=1}^{N}\left(1+\frac{\hat{s}^2}{\omega_{zn}^2}\right)}{\prod_{n=1}^{N}\left(1+\frac{\hat{s}^2}{\omega_{\alpha n}^2}\right)},\qquad N\to\infty. \tag{55}$$

Finally

$$G_{v\tau}(\hat{s}):=\frac{v(\ell,\hat{s})}{\tau(\hat{s})}=-\frac{11\ell^2}{40(1+3\varepsilon)EI}\cdot\frac{\hat{s}^2\prod_{n=1}^{\infty}\left(1+\frac{\hat{s}^2}{\omega_{\delta n}^2}\right)}{\hat{s}^2\prod_{n=1}^{\infty}\left(1+\frac{\hat{s}^2}{\omega_{\theta n}}\right)}, \tag{56}$$

where $\omega_{\delta n}=\beta_n^2$ and β_n $(n=1, 2, \cdots)$ are the real positive roots of

$$(\sinh\beta+\sin\beta)\beta^{-1}-(1+\cosh\beta\cos\beta)=0. \tag{57}$$

Although $G_{v\tau}(\hat{s})$ does not have nonminimum phase zeros, it is not well-behaved owing to the pole-zero cancellation at $\hat{s}=0$ (i.e. the lack of observability of the rigid body modes).

APPENDIX B

The infinite product expansions for transcendental functions used in this paper are summarized as follows.[2,17] In accordance with the context of this paper, $\hat{s}^2=-\beta^4$ is used whenever it is appropriate.

A1. $\sinh\beta+\sin\beta=2\beta\prod_{n=1}^{\infty}\left(1-\frac{\hat{s}^2}{\omega_{zn}^2}\right)$, $\omega_{zn}=2a_n^2$.

$\tanh a_n+\tan a_n=0$, $(a_n>0, \text{real})$.

$a_n=\left(n-\frac{1}{4}\right)\pi$ as $n\to\infty$.

$\omega_{z1}=2(2.365)^2$, $\omega_{z2}=2(5.498)^2$, $\omega_{z3}=2(8.639)^2$,
$\omega_{z4}=2(11.781)^2$, $\omega_{z5}=2(14.923)^2$, $\omega_{z6}=2(18.064)^2$.

A2. $1+\cosh\beta\cos\beta=2\prod_{n=1}^{\infty}\left(1+\frac{\hat{s}^2}{\omega_{pn}^2}\right)$, $\omega_{pn}=b_n^2$.

$\cosh b_n\cos b_n+1=0$, $(b_n>0, \text{real})$.

$b_n=\left(n-\frac{1}{2}\right)\pi$ as $n\to\infty$.

$\omega_{p1}=1.875^2$, $\omega_{p2}=4.694^2$, $\omega_{p3}=7.855^2$,
$\omega_{p4}=10.996^2$, $\omega_{p5}=14.137^2$, $\omega_{p6}=17.279^2$.

A3. $\cos\beta\sinh\beta-\sin\beta\cosh\beta$

$=-\frac{2}{3}\beta^3\prod_{n=1}^{\infty}\left(1+\frac{\hat{s}^2}{\omega_{\beta n}^2}\right)$, $\omega_{\beta n}=c_n^2$.

$\tanh c_n-\tan c_n=0$, $(c_n>0, \text{real})$.

$c_n=\left(n+\frac{1}{4}\right)\pi$ as $n\to\infty$.

$\omega_{\beta 1}=3.927^2$, $\omega_{\beta 2}=7.069^2$, $\omega_{\beta 3}=10.210^2$,
$\omega_{\beta 4}=13.352^2$, $\omega_{\beta 5}=16.493^2$, $\omega_{\beta 6}=19.635^2$.

A4. $\sin\beta\sinh\beta=\beta^2\prod_{n=1}^{\infty}\left(1+\frac{\hat{s}^2}{n^4\pi^4}\right)$.

Note that the asymptotic expressions are quite accurate (to three decimal places) for $n\ge 5$.

https://doi.org/10.1017/S0263574702004538 Published online by Cambridge University Press